A Two-Big-Leaf Model for Canopy Temperature, Photosynthesis, and Stomatal Conductance

YONGJIU DAI

School of Earth and Atmospheric Sciences, Georgia Institute of Technology, Atlanta, Georgia, and Research Center for Remote Sensing and GIS, Beijing Normal University, Beijing, China

ROBERT E. DICKINSON

School of Earth and Atmospheric Sciences, Georgia Institute of Technology, Atlanta, Georgia

YING-PING WANG

CSIRO Atmospheric Research, Aspendale, Victoria, Australia

(Manuscript received 23 May 2003, in final form 19 December 2003)

ABSTRACT

The energy exchange, evapotranspiration, and carbon exchange by plant canopies depend on leaf stomatal control. The treatment of this control has been required by land components of climate and carbon models. Physiological models can be used to simulate the responses of stomatal conductance to changes in atmospheric and soil environments. Big-leaf models that treat a canopy as a single leaf tend to overestimate fluxes of CO_2 and water vapor. Models that differentiate between sunlit and shaded leaves largely overcome these problems.

A one-layered, two-big-leaf submodel for photosynthesis, stomatal conductance, leaf temperature, and energy fluxes is presented in this paper. It includes 1) an improved two stream approximation model of radiation transfer of the canopy, with attention to singularities in its solution and with separate integrations of radiation absorption by sunlit and shaded fractions of canopy; 2) a photosynthesis–stomatal conductance model for sunlit and shaded leaves separately, and for the simultaneous transfers of CO_2 and water vapor into and out of the leaf—leaf physiological properties (i.e., leaf nitrogen concentration, maximum potential electron transport rate, and hence photosynthetic capacity) vary throughout the plant canopy in response to the radiation–weight time-mean profile of photosynthetically active radiation (PAR), and the soil water limitation is applied to both maximum rates of leaf carbon uptake by Rubisco and electron transport, and the model scales up from leaf to canopy separately for all sunlit and shaded leaves; 3) a well-built quasi-Newton–Raphson method for simultaneous solution of temperatures of the sunlit and shaded leaves.

The model was incorporated into the Common Land Model (CLM) and is denoted CLM 2L. It was driven with observational atmospheric forcing from two forest sites [Anglo-Brazilian Amazonian Climate Observation Study (ABRACOS) and Boreal Ecosystem–Atmosphere Study (BOREAS)] for 2 yr of simulation. The simulated fluxes by CLM 2L were compared with the observations, and with the results by the CLM with a single big-leaf scheme (CLM 1L) and by the CLM with the assimilation–stomatal conductance scheme of NCAR Land Surface Model (LSM). The results showed that CLM 2L was an improvement compared to the CLM 1L and the CLM for the test cases of tropical evergreen broadleaf land cover and coniferous boreal forest.

1. Introduction

Canopy models that link the terrestrial biosphere to atmosphere can be categorized as either multilayer or big-leaf models. A multilayer model integrates the fluxes from each layer to give the total flux (Wang and Jarvis 1990; Leuning et al. 1995); while the big-leaf approach maps properties of the whole canopy onto a single leaf to calculate the flux (e.g., Sellers et al. 1996a; Bonan 1996; Dickinson et al. 1998). These methods necessarily use different parameterizations for the nonlinear relationships that govern assimilation and transpiration. The multilayer models can use parameters that are measured at the leaf level. The big-leaf models require parameters at the canopy level that cannot be measured directly, nor defined as the arithmetic mean of leaf-level parameters because of nonlinearity (McNaughton 1994; Wang et al. 2001). Rather, they require some plausible assumption about the vertical profile of leaf properties such as the Rubisco enzyme. This is commonly determined through the hypothesis that the limiting rate of carbon uptake V_{max} should vary with canopy depth as

Corresponding author address: Dr. Yongjiu Dai, Research Center for Remote Sensing and GIS of School of Geography, Beijing Normal University, No. 19, Xinjiekouwai St., Beijing 100875, China.
E-mail: yongjiudai@bnu.edu.cn

the photosynthetically active radiation (PAR; e.g., Sellers et al. 1992). With such an assumption, canopy properties, such as V_{max} and potential electron transport rate J_{max} can be related to the corresponding measurable properties of the leaves at the canopy top.

Big-leaf models have been extensively used in land surface climate modeling (Sellers et al. 1996a; Bonan 1996; Dickinson et al. 1998; Dai et al. 2003). They require fewer parameters and are more economical in computer time than the multilayer models. They treat the canopy as single big leaf with the fluxes of leaf energy, water, and CO_2 calculated by coupled equations. The models of Bonan (1996) and Dickinson et al. (1998) treat the assimilation and stomatal conductance of sunlit leaves separately from that of shaded leaves but use a single leaf temperature.

Wang and Leuning (1998) developed a more comprehensive two-leaf approach with the canopy described by variables and parameters that represent the bulk properties of all sunlit or shaded leaves, using the Goudriaan and van Larr (1994) radiation model to estimate the total amount of radiation in visible, near-infrared, and thermal bands. Conductances of the stomata and leaf boundary layer are also integrated over all the sunlit and shaded leaves separately. They compared the fluxes of CO_2, water vapor, and sensible heat as predicted by their two-leaf model with those of a multilayered model, and found no significant differences in their predictions. The two-leaf model has recently been refined to further improve the agreement in the predicted fluxes between the two-leaf model and a multilayered canopy model (Wang 2000). Wang (2003) showed that the fluxes predicted by the two-leaf model with Goudriaan and van Larr's radiation are very similar (relative differences $<5\%$) to those by the two-leaf model using the two-stream approximation (Sellers 1985). Wang and Leuning (1998) derived the physiological and physical properties for both sunlit and shaded leaves similar to the approach of Sellers et al. (1992, 1996a), but considered sunlit and shaded leaves separately. Other differences between Wang and Leuning's two-leaf model and Seller's one big-leaf model are use of a different stomatal model, allowing for decoupled vegetation (see Raupach 1995).

The leaf biochemical processes depend on PAR and leaf temperature. Direct sunshine heats leaves more than the scattered light in the shade, and hence sunlit leaves can be several degrees warmer than shaded leaves under sunny and dry conditions. Leaves that are most frequently shaded are thinner than those in the sun. Both the epidermal and mesophyll tissues are thicker in sunlit leaves, and the number of cells per unit leaf volume is higher. Morpho-anatomical and physiological adaptations allow the chestnut to optimize its use of the limited radiant energy available, but shading greatly reduces productivity (Boardman 1977). The net photosynthetic rate A_n of sunlit leaves is relatively high due to light saturation but there is a drastic reduction in A_n with the low light levels of shaded leaves. If such differences in physiological properties of leaves and the differences in PAR and temperatures between sunlit and shaded leaves are neglected, the estimates of photosynthesis and energy fluxes for the canopy may be significantly in error. Photosynthesis of shaded leaves has an essentially linear response to absorbed PAR, while photosynthesis of sunlit leaves is often light saturated and so independent of absorbed PAR. Hence the averaging of PAR in each of these two classes of leaves, sunlit and shaded, is appropriate and should introduce little error in the final predicted canopy photosynthesis. This concept (Sinclair et al. 1976) has been introduced into land surface modeling by de Pury and Farquhar (1997), Wang and Leuning (1998).

Leaves change their position with wind and the sun during the day causing the surfaces in direct sun (sunflecks) to move around. Leaves require on the order of 3–20 min for opening stomata and 12–35 min for closing stomata (Woods and Turner 1971; Sellers 1985). Leaves change their temperatures over similar time scales or shorter. Thus, over the typical model time step, it is appropriate to assume leaf stomatal function and temperatures have equilibrated to light levels as assumed in the separation into sunlit and shaded fractions.

We have developed a submodel for assimilation and stomatal conductance with two big leaves that treats the leaf temperatures and fluxes (energy, water, and CO_2) separately for sunlit and shaded fractions of canopy. The submodel formulations and parameters are described in section 2. The submodel was incorporated into the Common Land Model (CLM) and run for two forest sites for 2 yr with the observed meteorological forcings. The simulated fluxes and leaf temperatures were evaluated with the observations and compared with what were obtained by CLM with a single big-leaf submodel and CLM with a National Center for Atmospheric Research (NCAR) Land Surface Model (LSM) scheme, as presented in section 4.

2. Model description

Canopy photosynthesis is modeled by equations describing the fluxes of both CO_2 and water vapor at the leaf level, and some method of scaling from leaf to canopy. Leaf-level responses require some form of parameterization of both the biochemistry within chloroplasts and the stomatal response to the environment. Most canopy gas exchange models employ the leaf biochemical model of photosynthesis by Farquhar et al. (1980) and some form of empirical stomatal response (Ball 1988; Leuning et al. 1995). In this section, we give the expressions used for the fraction of sunlit and shaded leaves, energy balance, radiative transfer, the photosynthesis and stomatal conductance for sunlit and shaded leaves separately, and their scaling up from leaf to canopy.

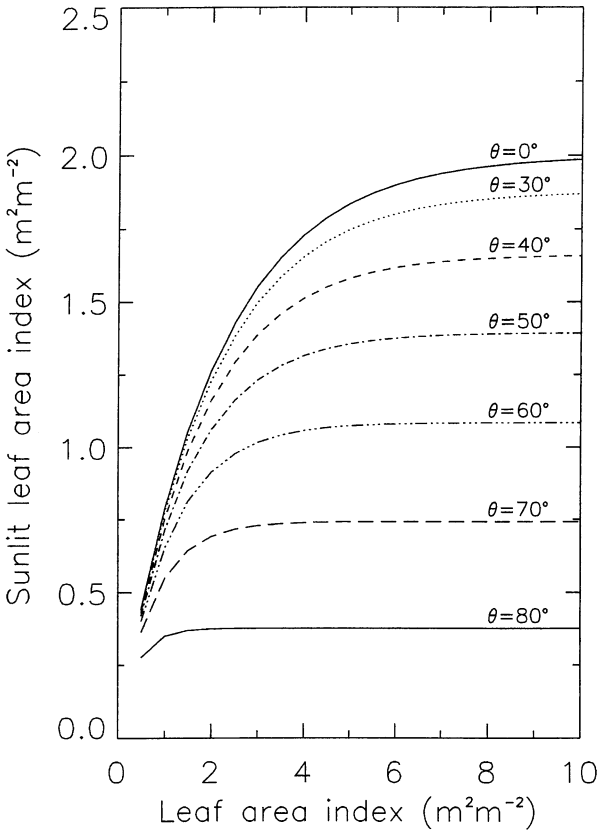

FIG. 1. Leaf area index of sunlit fraction of canopy [Eq. (3)] for the case of leaves with random distribution of leaf angles [i.e., $G(\mu) = 0.5$], θ is solar zenith angle.

a. Fraction of sunlit/shaded leaves

Leaves are sunlit leaf area if not shaded in the direction of the sun. The fractional area over which this occurs decreases exponentially with the cumulative leaf area index from the canopy top. The fractions of sunlit and shaded leaves at a canopy depth x, f_{Sun}, and f_{Sha}, are calculated from

$$f_{\text{Sun}}(x) = e^{-k_b x}; \qquad f_{\text{Sha}} = 1 - f_{\text{Sun}}, \tag{1}$$

where x is the cumulative leaf area index measured downwards from the top of the canopy, k_b is the direct beam extinction coefficient of the canopy and

$$k_b = G(\mu)/\mu, \tag{2}$$

where $G(\mu) = \phi_1 + \phi_2\mu$, $\phi_1 = 0.5 - 0.633\chi - 0.33\chi^2$, $\phi_2 = 0.877(1 - 2\phi_1)$, and χ is an empirical parameter related to the leaf angle distribution, varying from -1 to 1 (1 for horizontal leaves, -1 for vertical leaves, and 0 for a spherical leaf angle distribution), and μ is the cosine of solar zenith angle. The leaf area index of sunlit and shaded fraction of canopy are calculated by integrating (1):

$$L_{\text{Sun}} = \int_0^{L_{\text{AI}}} f_{\text{Sun}}(x)\, dx = \frac{1}{k_b}(1 - e^{-k_b L_{\text{AI}}});$$

$$L_{\text{Sha}} = L_{\text{AI}} - L_{\text{Sun}}. \tag{3}$$

The sunlit and shaded fractions of the canopy are

$$F_{\text{Sun}} = L_{\text{Sun}}/L_{\text{AI}}; \qquad F_{\text{Sha}} = L_{\text{Sha}}/L_{\text{AI}}. \tag{4}$$

This division into sunlit and shaded leaves is important in scaling canopy processes, because the sunlit leaves will receive a much higher light flux density than shaded leaves under sunny conditions. The possible importance of such leaf orientation effects as discussed by Sinclair et al. (1976) and Norman (1979) is not considered here. Figure 1 calculates the variation of the sunlit fraction of a canopy with solar angle θ. The sunlit fraction decreases significantly for $\theta > 30°$ and reaches constant values for leaf area index greater than 5. The L_{Sun} calculated by Eq. (3) is in reasonable agreement with the measurements by Kucharik et al. (1998): typically, L_{Sun} in aspen ($L_{\text{AI}} = 3.3$) range between 0.8–1.0 at a 70° sun angle and 1.1–1.6 at a 30° sun angle. The canopy keeps a considerable percentage of leaves in shade at all solar angles with a minimum fraction $F_{\text{Sha}} = 20\%$ for $L_{\text{AI}} = 1$ to $F_{\text{Sha}} = 60\%$ for $L_{\text{AI}} = 5$.

b. Equations of leaf temperatures and fluxes

1) LEAF TEMPERATURE OF SUNLIT/SHADED FRACTION OF CANOPY

Leaf temperatures are determined by the canopy energy budget equations for sunlit and shaded fractions of canopy as follows:

$$C_c \frac{\partial [T_l]_j}{\partial t} = 0 = [I_s]_j + [I_{\text{ir}}]_j - [H_c]_j - L[E_c]_j. \tag{5}$$

Hereafter, the subscript "j" denotes the sunlit ($j = 1$) and shaded ($j = 2$) fraction of canopy, respectively; $[\,]_{j=1}$ and $[\,]_{j=2}$ denote the integration for sunlit and shaded fractions of canopy, respectively, that is, $\int_0^{L_{\text{AI}}} [\,] f_{\text{Sun}}\, dx$ and $\int_0^{L_{\text{AI}}} [\,] f_{\text{Sha}}\, dx$, but for temperatures and partial pressures, they mean the bulk (averaged) values. The value C_c is the canopy heat capacity (J m^{-2} K^{-1}) and is assumed to be negligible, I_s is the summed net solar radiation absorbed by sunlit and shaded fraction of canopy (W m^{-2}), I_{ir} is the net longwave radiation absorbed by sunlit/shaded fractions of canopy (W m^{-2}), H_c is the sensible heat flux from foliages to canopy air (W m^{-2}), E_c is the moisture fluxes (transpiration and evaporation of intercepted water) from leaves to canopy air (kg m^{-2} s^{-1}). The equations are

$$[H_c]_{j=1} = \rho c_p L_{\text{Sun}} \frac{[T_l]_{j=1} - T_{\text{af}}}{[r_b]_{j=1}} \tag{6a}$$

$$[H_c]_{j=2} = \rho c_p (L_{\text{Sha}} + S_{\text{AI}}) \frac{[T_l]_{j=2} - T_{\text{af}}}{[r_b]_{j=2}} \tag{6b}$$

$$[E_c]_{j=1} = \rho\left\{\delta_1(1 - f_{\text{wet}})L_{\text{Sun}}\frac{1}{[r_b]_{j=1} + [r_s]_{j=1}} + \{1 - \delta_1(1 - f_{\text{wet}})\}L_{\text{Sun}}\frac{1}{[r_b]_{j=1}}\right\} \times \{q_{\text{sat}}([T_l]_{j=1}) - q_{\text{af}}\} \quad (7a)$$

$$[E_c]_{j=2} = \rho\left\{\delta_2(1 - f_{\text{wet}})L_{\text{Sha}}\frac{1}{[r_b]_{j=2} + [r_s]_{j=2}} + \{1 - \delta_2(1 - f_{\text{wet}})\}(L_{\text{Sha}} + S_{\text{AI}})\frac{1}{[r_b]_{j=2}}\right\} \times \{q_{\text{sat}}([T_l]_{j=2}) - q_{\text{af}}\}, \quad (7b)$$

where ρ and c_p is the density and specific heat of air (kg m^{-3}, J kg^{-1} K^{-1}), respectively; δ_1 and δ_2 is the step functions for sunlit and shaded leaves, respectively, and 1 for positive argument and 0 for negative argument of $\{q_{\text{sat}}([T_l]) - q_{\text{af}}\}$; S_{AI} is the dead leaf or stem area index; f_{wet} is fraction of wet leaves; r_b is the averaged (bulk) leaf boundary layer resistance (s m^{-1}); r_s is the averaged leaf stomatal resistance (s m^{-1}); q_{sat} (T_l) is the saturated specific humidity (kg kg^{-1}) at temperature T_l; T_l is the leaf temperature of canopy. Here, T_{af} and q_{af} are the temperature and specific humidity of canopy space air, respectively, (K, kg kg^{-1}).

The air within the canopy has negligible heat capacity and so heat flux from foliage $[H_c]_{j=1}$, $[H_c]_{j=2}$ and from the ground H_g must be balanced by heat flux to atmosphere H_a, that is,

$$H_a = H_g + [H_c]_{j=1} + [H_c]_{j=2}. \quad (8)$$

Similarly, the canopy air is assumed to have zero capacity for water vapor storage so that the flux of water from canopy air E_a balances the flux from foliage $[E_c]_{j=1}$ and $[E_c]_{j=2}$, and the flux from the ground, E_g, that is,

$$E_a = E_g + [E_c]_{j=1} + [E_c]_{j=2}. \quad (9)$$

Here, T_{af} and q_{af} (or e_a) are updated by (8) and (9) within the iterative procedure for leaf temperature calculations, respectively. The numerical solution of Eq. (5) is described in appendix C.

N.B., the equations for r_b, E_a, E_g, H_a, and H_g are exactly the same as that in the CLM (http://climate.eas.gatech.edu/dickinson).

2) CO_2 BALANCE

The CO_2 flux budget within the canopy can be described by a CO_2 concentration conservation equation:

$$C_{\text{CO}_2}\frac{\partial c_a}{\partial t} = 0 = -F_c - [A_n]_{j=1} - [A_n]_{j=2} + R_p + R_{\text{soil}}. \quad (10)$$

In this study, the CO_2 storage (C_{CO_2}) within canopy air is assumed to be negligible. The value R_{soil} is the CO_2 flux from soil surface to canopy air; R_p is the nonleaf plant respiration, which was taken as zero in this study. Here, $[A_n]_j$ is the net CO_2 assimilation of canopy by sunlit ($j = 1$) or shaded leaves ($j = 2$), and can be written as

$$[A_n]_j = ([g_b]_j/1.37)(c_a - [c_s]_j). \quad (11)$$

The value F_c is the CO_2 flux from canopy to atmosphere, and can be written

$$F_c = (g_a/1.37)(c_a - c_m), \quad (12)$$

where c_s, c_a, and c_m are the mixing ratio of CO_2 in air at leaf surface, canopy air space and atmosphere reference height, respectively. Here, g_a is aerodynamic conductance of water vapor between reference height and canopy air space, $[g_b]_j$ is the bulk leaf boundary conductance ($j = 1$ for sunlit and $j = 2$ for shaded).

c. Radiation absorption

1) SOLAR RADIATION

The two-stream approximation for the radiation transfer within a canopy (Dickinson 1983; Sellers et al. 1985) is used to describe the interception, reflection, transmission, and absorption of radiation by vegetation and soil using standard parameterizations for soil and snow albedos (Dickinson et al. 1993). The solutions for singularity points, not previously considered, are provided in appendix A.

It is assumed that shaded leaves receive diffuse light only, sunlit leaves receive both diffuse and direct radiation (Spitters et al. 1986). The solar radiation flux density absorbed by the sunlit leaves in the canopy is given as the sum of components of direct-beam I_{lb}, scattered direct-beam I_{lbs}, and diffuse radiation I_{ld}. That is,

$$[I_s]_{j=1} = \int_0^{L_{\text{AI}}} \{I_{\text{lb}} + (I_{\text{lbs}} + I_{\text{ld}})f_{\text{Sun}}\}\, dx. \quad (13a)$$

Solar radiation flux density absorbed by the shaded leaves in the canopy is given as the sum of components of scattered direct-beam I_{lbs} and diffuse radiation I_{ld}:

$$[I_s]_{j=2} = \int_0^{L_{\text{AI}}} (I_{\text{lbs}} + I_{\text{ld}})f_{\text{Sha}}\, dx. \quad (13b)$$

The direct incident beam radiation absorbed by leaves at canopy depth x (per unit leaf area index)—excluding scattering, I_{lb}, is obtained from the exponential light profile with the complementary transmission as

$$I_{\text{lb}} = (1 - \omega)k_b e^{-k_b x} I_{b0}. \quad (14)$$

The scattered direct-beam radiation absorbed by leaves at canopy depth x, I_{lbs}, is given by

$$I_{\text{lbs}} = \left\{\omega k_b e^{-k_b x} + \frac{d(I^{\uparrow}_{\text{dir}} - I^{\downarrow}_{\text{dir}})}{dx}\right\} I_{b0}, \quad (15)$$

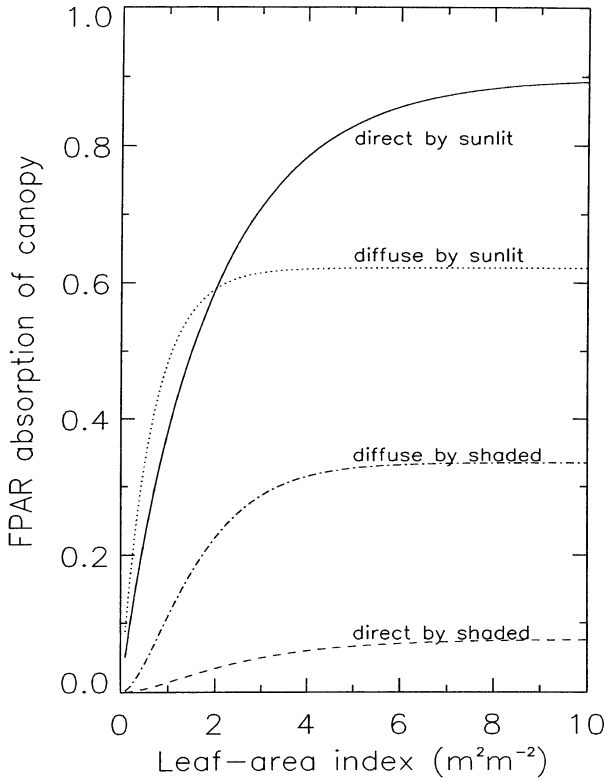

FIG. 2. Absorption of PAR by sunlit/shaded fraction of canopy for direct and diffuse incident of PAR radiation [Eqs. (13a)–(13b)]; the values are as the fractions related to the incident PAR (divided by incident direct and diffuse, respectively), where $\chi = 0$, $\omega = 0.15$, $\theta = 0°$.

where $I^{\uparrow}_{\text{dir}}$, $I^{\downarrow}_{\text{dir}}$ are the upward and downward diffuse fluxes of the scattered direct-beam radiation, respectively, normalized by the incident direct-beam radiation above the canopy. The first term is the direct-beam flux penetrating to the specified cumulative leaf area depth x in the canopy without scattering; the second term is the change of net upward of scattered direct-beam radiation flux. Here, I_{b0} is the incident direct-beam radiation above the canopy, I_{d0} is the incident diffuse radiation above the canopy. The total amount of incident diffuse and scattered diffuse radiation absorbed by canopy depth x, I_{ld}, is given by

$$I_{\text{ld}} = \frac{d(I^{\uparrow}_{\text{dif}} - I^{\downarrow}_{\text{dif}})}{dx} I_{d0}, \tag{16}$$

where $I^{\uparrow}_{\text{dif}}$, $I^{\downarrow}_{\text{dif}}$ are the upward and downward diffuse fluxes of incident diffuse radiation and scattered diffuse radiation, respectively, normalized by the incident diffuse solar flux density above the canopy. Total absorbed flux density of incident solar radiation by the canopy is

$$[I_s] = [I_s]_{j=1} + [I_s]_{j=2}. \tag{17}$$

The calculations of Eqs. (13)–(17) are performed for visible and near-infrared components separately.

Figure 2 shows how the PAR absorptions by sunlit and shaded fractions of canopy vary with leaf area index. It is clear that the near maximum absorption of PAR as calculated by Eqs. (13a)–(13b) are achieved in the range of 4–5. Also, the effect of solar incident pattern (direct/diffuse) is significant, it is important to discriminate between the direct and diffuse components of solar incident. Sunlit leaves absorb the major portion of both the direct and diffuse component of solar visible fluxes, only a very low portion of direct beam is absorbed by shaded leaves (<5%). Thus the PAR absorption of direct beam by shaded leaves commonly has been ignored, such as in the NCAR LSM (Bonan 1996). The sum of the direct and diffuse terms add up to 0.96 and 0.95, respectively. The remaining radiation has contributed to the albedo.

2) LONGWAVE RADIATION

The net absorbed thermal radiation does not account for different canopy location of the sunlit versus shaded leaves, but are calculated by

$$[I_{\text{ir}}]_{j=1} = (L_a\delta_t - 2\sigma[T_l]^4_{j=1}\delta_t + \delta T^4_g\delta_t)F_{\text{Sun}}, \quad \text{for sunlit leaves} \tag{18a}$$

$$[I_{\text{ir}}]_{j=2} = (L_a\delta_t - 2\sigma[T_l]^4_{j=2}\delta_t + \sigma T^4_g\delta_t)F_{\text{Sha}}, \quad \text{for shaded leaves,} \tag{18b}$$

where L_a is the incident thermal infrared radiation, δ_t is the fraction of longwave radiation absorbed by canopy and $\delta_t = 1 - e^{-L_{\text{AI}}}$, σ is the Stefan–Boltzmann constant (W m^{-2} K^{-4}), T_g is the ground temperature (K).

d. Canopy photosynthesis and stomatal conductance

1) LEAF PHOTOSYNTHESIS AND STOMATAL CONDUCTANCE

This paper addresses how temperatures for sunlit and shaded fractions of canopy can be distinguished and photosynthesis aggregated from leaf to canopy. We use the leaf photosynthesis–stomatal conductance model [second version of Simple Biosphere Model (SiB2)] of Sellers et al. (1996a) that implemented the photosynthesis model of Farquhar et al. (1980), as formulated by Collatz et al. (1992) and relating stomatal conductance to carbon assimilation according to Ball (1988). This approach is summarized with modifications in Table 1. The symbols and definitions of parameters are listed in Table 2. Three modifications were made in 1) electron transport rate J, 2) soil water stress on maximum catalytic capacity of Rubico V_{max}, and 3) potential electron transport rate J_{max}.

The value V_m is the maximum catalytic capacity of Rubisco at saturating levels of Ribulose bisphosphate (RuBP) and intercellular partial pressure of CO_2, (mol m^{-2} s^{-1}), which varies with leaf temperature and soil water:

TABLE 1. Equations of the leaf photosynthesis and stomatal conductance model.

Equation	Definition	
Photosynthesis rate:		
$A_n = A - R_d$	Net assimilation (mol m^{-2} s^{-1})	(19)
$A = \min(w_c, w_e, w_s)$	Leaf assimilation rates (mol m^{-2} s^{-1})	(20)
$w_c = \begin{cases} V_m\left\{\dfrac{c_i - \Gamma^*}{c_i + K_c(1 + O_2/K_o)}\right\}, & \text{for } C_3 \\ V_m, & \text{for } C_4 \end{cases}$	Rubisco (leaf enzyme) limited rate of assimilation (mol m^{-2} s^{-1})	(21)
$w_e = \begin{cases} J\dfrac{c_i - \Gamma^*}{(c_i + 2\Gamma^*)}, & \text{for } C_3 \\ J, & \text{for } C_4 \end{cases}$	Light-limited rate of assimilation (mol m^{-2} s^{-1})	(22)
$w_s = \begin{cases} 0.5V_m, & \text{for } C_3 \\ 2 \times 10^4 V_m c_i/p, & \text{for } C_4 \end{cases}$	Carbon compound export limitation (C_3 plants), or PEP-carboxylase (C_4) limitation on photosynthesis (mol m^{-2} s^{-1})	(23)
$R_d = f_d f_T(T_1)$	Dark respiration rate, f_d, is the dark respiration of leaf at 20°C (mol m^{-2} s^{-1})	(24)
$A_n - g_s$ model:		
$g_s = m\dfrac{A_n}{c_s}h_s p + b$	A semiempirical model for photosynthesis and stomatal conductance	(25)
H_2O and CO_2 exchanges with external environment:		
$E_{tr} \propto g_l(e_s - e_a) = g_s(e_i - e_s)$	H_2O flux (kg m^{-2} s^{-1})	(26)
$A_n = \dfrac{c_a - c_s}{p}\dfrac{g_l}{1.37} = \dfrac{c_s - c_i}{p}\dfrac{g_s}{1.6}$	CO_2 flux (mol m^{-2} s^{-1})	(27)

where

g_s = leaf stomatal conductance (mol m^{-2} s^{-1});
g_l = leaf boundary conductance (mol m^{-2} s^{-1});
m = empirical coefficient from observations;
b = empirical coefficient from observations (mol m^{-2} s^{-1});
p = atmospheric pressure at surface (Pa);
O_2 = partial pressure of O_2 in leaf interior (Pa);
h_s = relative humidity at leaf surface;
e_a, e_s, e_i = partial pressure of H_2O in canopy air space, at the leaf surface, and inside the leaf (saturated) (Pa), respectively;
c_a, c_s, c_i = partial pressure of CO_2 in canopy air, at leaf surface, and interior leaf (Pa), respectively;
1.37, 1.6 = ratio of the diffusivities of H_2O and CO_2 in the leaf boundary and stomatal pores, respectively.

TABLE 2. Biome physiological parameters.

Parameter	Symbol	Unit
Biome dependent		
Maximum Rubisco capacity at top canopy at 25°C per leaf area	V_{cmax}	mol m^{-2} s^{-1}
Intrinsic quantum yield epsilon	ε	mol mol^{-1}
Stomatal slope factor	m	—
Minimum stomatal conductance	b	mol m^{-2} s^{-1}
One-half point of high temperature inhibition function	s_2	K
One-half point of low temperature inhibition function	s_4	K
Coefficient of leaf nitrogen allocation within canopy	k_n	—
Biome independent		
CO_2 compensation point	$\Gamma^* = 0.5O_2/S$	Pa
Rubisco Michaels–Menten constant for CO_2	$K_c = 30 \times 2.1^{Q_{10}}$	Pa
Rubisco inhibition constant for oxygen	$K_o = 30\,000 \times 1.2^{Q_{10}}$	Pa
Rubisco specificity for CO_2 relative to oxygen	$S = 2600 \times 0.57^{Q_{10}}$	Pa
Q_{10} temperature coefficient	$Q_{10} = (T_l - 298.16)/10$	—
Slope of high temperature inhibition function	$s_1 = 0.3$	K^{-1}
Slope of low temperature inhibition function	$s_3 = 0.2$	K^{-1}
Slope of high temperature inhibition function (leaf respiration)	$s_5 = 1.3$	K^{-1}
One-half point of high temperature inhibition function (leaf respiration)	$s_6 = 328.16$	K

$$V_m = V_{\max} f_T(T_l) f_w(\theta), \tag{28}$$

where $V_{\max}$ is the V_m in the presence of saturating soil water and at temperature 25°C, and is assumed to be a function of leaf nitrogen as over 20% of leaf nitrogen is invested in Rubisco. The temperature dependence $f_T(T_l)$ of V_m are calculated as follows:

$$f_T(T_l) = \begin{cases} \dfrac{2.1^{Q_{10}}}{\{1 + e^{s_1(T_l - s_2)}\}} & \text{for } C_3 V_m \\ \dfrac{2.1^{Q_{10}}}{(\{1 + e^{s_1(T_l - s_2)}\}/\{1 + e^{s_3(s_4 - T_l)}\})} & \text{for } C_4 V_m \end{cases} \tag{29}$$

$$f_T(T_l) = 2.1^{Q_{10}}/\{1 + e^{s_5(T_l - s_6)}\}, \quad \text{for } R_d V_m. \tag{30}$$

Here, J is the electron transport rate for a given absorbed photon radiation I_s, and related to the minimum of the potential maximum (light saturated) electron transport rate $0.25J_{\max}$ and the PAR absorbed by photosystem II, εI_s. Usually, J is described by a nonrectangular hyperbolic function: $\beta J^2 - (\varepsilon I_s + 0.25J_{\max})J + 0.25\varepsilon I_s J_{\max} = 0$ (Smith 1937; Farquhar and Wong 1984; Wang and Polglase 1995) to smooth the transition. In SiB2 (Sellers et al. 1992, 1996a), it was only related to the PAR absorption with no maximum limit. To permit J to be integrable analytically over the canopy leaf area, the simpler relation is taken in this model, that is,

$$J = \min(\varepsilon I_s, J_m/4). \tag{31}$$

Here, I_s refers to the PAR absorbed by the leaf (mol m^{-2} s^{-1}) and ε is the quantum yield of electron transport; J_m is potential electron transport rate (mol m^{-2} s^{-1}), which varies with leaf temperature and soil water (Tezara et al. 1999),

$$J_m = J_{\max} f_T(T_l) f_w(\theta). \tag{32}$$

The modifier, $f_w(\theta)$, is newly implemented to reduce $J_{\max}$ as done for $V_{\max}$, when soil water is limiting (Wang et al. 2001). The temperature dependence $f_T(T_l)$ of J_m is adopted from de Pury and Farquhar (1997) as

$$f_T(T_l) = \frac{\exp\{10Q_{10}E_a/(RT_l298)\}(1 + \exp\{(298S - H)/(298R)\})}{(1 + \exp\{(ST_l - H)/(RT_l)\})}, \quad \text{for } J_m. \tag{33}$$

Here, $H = 220 \times 10^3$ J mol^{-1} as a curvature parameter for $J_{\max}$; $R = 8.314$ J mol^{-1} K^{-1}, the universal gas constant; $S = 710$ J K^{-1} mol^{-1}, the electron-transport temperature response parameter; $E_a = 37\,000$ J mol^{-1}, the activation energy.

The effect of soil water stress on assimilation is assumed given by

$$f_w(\theta) = \sum_1^n f_{\text{root},j}\left(\frac{\psi_{\max} - \psi_j}{\psi_{\max} - \psi_{\text{fc}}}\right). \tag{34}$$

Here, n is the total number of soil layers, subscript j is the number of soil layer. The value $f_{\text{root},j}$ is the root fraction within soil layer j, $\psi_{\max}$ is the maximum value of soil matrix potential before leaves wilt (-1.5×10^5 mm), ψ_{fc} is the soil matrix potential at filed capacity, the factor $(\psi_{\max} - \psi)/(\psi_{\max} - \psi_{\text{fc}})$ ranges from 0 at the permanent wilting point to 1 at field capacity.

2) SCALING UP FROM LEAF TO CANOPY

The Eqs. (19)–(27) are applied to a single leaf with known physiological, physical properties, and forcing conditions. The next step is to integrate these equations to describe the canopy photosynthesis $[A_n]_j$ and stomata conductance $[g_s]_j$.

The maximum Rubisco capacity $V_{\max}$ could be correlated with a measurement of leaf nitrogen concentration N_1. A linear relationship between $V_{\max}$ and N_1 is commonly assumed (Field 1983; Leuning et al. 1991; Harley et al. 1992) with a residual leaf nitrogen content N_b (a threshold value of leaf nitrogen content below which there is no photosynthesis, when $V_{\max} = 0$), that is, $V_{\max} = \chi_n(N_1 - N_b)$, in which χ_n is the ratio of Rubisco capacity to leaf nitrogen, could be used to relate $V_{\max}$ (from leaf photosynthesis measurements) to measurements of N_1. The vertical profile of leaf nitrogen has been modeled as decreasing exponentially with cumulative relative leaf area index, x, from the top of the canopy (Hirose and Werger 1987; Leuning et al. 1995; de Pury and Farquhar 1997), that is, $N_1(x) = (N_0 - N_b)\exp(-k_n x) + N_b$, where N_0 is the nominal leaf nitrogen content at the top of the canopy, k_n is the coefficient of leaf nitrogen allocation. Hence, the Rubisco capacity $V_{\max}$ is given by

$$V_{\max} = V_{c\max} \exp(-k_n x), \tag{35}$$

where $V_{c\max}$ is for leaves at the top of the canopy at 25°C, and $V_{c\max} = \chi_n(N_0 - N_b)$.

The potential electron transport, $J_{\max}$, within the canopy was assumed to be proportional to $\exp(-k^*_{d,1}x)$ (Wang and Polglase 1995; Wang and Leuning 1998), that is, it decreases exponentially from the top to the bottom of the canopy, that is,

$$J_{\max} = J_{c\max} \exp(-k^*_{d,1}x), \tag{36}$$

where $k^*_{d,1}$ is the extinction coefficients for diffuse PAR; $J_{c\max}$ is for leaves at the top of the canopy at 25°C, the relationship of $V_{c\max}$ and $J_{c\max}$ has been widely investigated by Wohlfahrt et al. (1999) who found that a fixed

value of $J_{c\max}/V_{c\max} = 2.1$ could be applied to a wide variety of leaves.

The equations for leaf-level photosynthesis and stomatal conductance can now be integrated over the depth of the canopy to yield bulk canopy values of $[A]_j$ and $[g_s]_j$ for sunlit and shaded fractions of canopy individually. This is done by the following:

1) Common (canopy average or bulk) $[c_l]_j$, $[c_s]_j$, $[e_s]_j$ and leaf temperature $[T_l]_j$ for sunlit/shaded leaves, respectively, are assumed.
2) Equation (35) is inserted into (21), (23), and (24) via (28); and (21), (23), and (24) are integrated over the depth of the canopy for sunlit and shaded fractions of canopy. Essentially, these integrations are only needed for the $V_{\max}$, and photosynthetic capacity of the sunlit and shaded leaf-fractions of the canopy are calculated as the integrals, respectively,

$$[V_{\max}]_{j=1} = \int_0^{L_{\mathrm{AI}}} V_{\max}(x) f_{\mathrm{Sun}}(x)\, dx = V_{c\max}\{1 - e^{-(k_n+k_b)L_{\mathrm{AI}}}\}\frac{1}{k_n + k_b} \tag{37a}$$

$$[V_{\max}]_{j=2} = \int_0^{L_{\mathrm{AI}}} V_{\max}(x) f_{\mathrm{Sha}}(x)\, dx = V_{c\max}\left(\{1 - e^{-k_n L_{\mathrm{AI}}}\}\frac{1}{k_n} - \{1 - e^{-(k_n+k_b)L_{\mathrm{AI}}}\}\frac{1}{k_n + k_b}\right). \tag{37b}$$

3) Equation (36) is inserted into (22) via (31), and integrated over the depth of the canopy for sunlit and shaded fractions of canopy. The integration for absorbed PAR was given by (13), and the integrations for potential electron transport J_m over sunlit and shaded leaf-fractions of the canopy are calculated as the integrals, respectively,

$$[J_{\max}]_{j=1} = \int_0^{L_{\mathrm{AI}}} J_{\max}(x) f_{\mathrm{Sun}}(x)\, dx = J_{c\max}\{1 - e^{-(k^*_{d,1}+k_b)L_{\mathrm{AI}}}\}\frac{1}{k^*_{d,1} + k_b}, \tag{38a}$$

$$[J_{\max}]_{j=2} = \int_0^{L_{\mathrm{AI}}} J_{\max}(x) f_{\mathrm{Sha}}(x)\, dx = J_{c\max}\left\{(1 - e^{-k^*_{d,1}L_{\mathrm{AI}}})\frac{1}{k^*_{d,1}} - \{1 - e^{-(k^*_{d,1}+k_b)L_{\mathrm{AI}}}\}\frac{1}{k^*_{d,1} + k_b}\right\}. \tag{38b}$$

4) For avoiding abrupt transition, the assimilation rate terms are described by combining into two quadratic equations, which are then solved for the smaller roots:

$$\beta_{cj}[w_p]_j^2 - [w_p]_j([w_c]_j + [w_e]_j) + [w_c]_j[w_e]_j = 0 \tag{39}$$

$$\beta_{ps}[A]_j^2 - [A]_j([w_p]_j + [w_s]_j) + [w_p]_j[w_s]_j = 0. \tag{40}$$

The canopy photosynthesis curvature factors β_{cj} and β_{ps} are assumed to be 0.877 and 0.99. The net assimilations of leaves are

$$[A_n]_j = [A]_l - [R_d]_j \tag{41}$$

5) The integrals of Eq. (25) are written by

$$[g_s]_j = m\frac{[A_n]_j}{[c_s]_j}\frac{[e_s]_j}{[e_i]_j}p_s + [b^*]_j, \tag{42}$$

where $b^* = bf_w(\theta) \times$ leaf area index of sunlit/shaded fraction of canopy. Equation (42) was converted to a quadratic equation of $[g_s]_j$, and solved for the larger roots.

The bulk canopy values of the partial pressures of CO_2 ($[c_l]_j$ and $[c_s]_j$) and leaf surface relative humidity $[h_s]_j = [e_s]_j/[e_i]_j$ are linked to conditions in the canopy air space through the canopy stomatal conductance $[g_s]_j$, the bulk canopy boundary layer conductance $[g_b]_j$, the net flux of CO_2 $[A_n]_j$ [Eq. (27)], and the transpiration [Eq. (26)], and are given by

$$[c_s]_j = c_a - 1.37[A_n]_j p_s/[g_b]_j,$$
$$[c_i]_j = [c_s]_j - 1.6[A_n]_j p_s/[g_s]_j, \tag{43}$$

$$[e_s]_j = \frac{[g_b]_j[e_i]_j + [g_s]_j e_a}{[g_b]_j + [g_s]_j}, \tag{44}$$

where $[g_b]_j$ is the bulk leaf boundary conductance, $[g_s]_j$ is the canopy stomata conductance, $[e_i]_j$ is water vapor pressure at interior leaf and taken as the saturated value (temperature T_l dependence only).

The unit of $[g_s]_j$ was converted from mol m^{-2} s^{-1} to m s^{-1} before used by equations (7a) and (7b):

$$1\ (\mathrm{m\ s^{-1}}) = 0.0224\frac{[T_l]_j}{273.16}\frac{1.013 \times 10^5}{p_s}\ (\mathrm{mol\ m^{-2}\ s^{-1}}) \tag{45}$$

The success of scaling up photosynthesis largely depends on biochemical properties in one-layered canopy models. The maximum Rubisco activity $V_{\max}$ was assumed to be linearly related to the leaf nitrogen, and that the nitrogen allocation was assumed to decline exponentially with cumulative L_{AI}. The potential electron transport $J_{\max}$ has been found to be closely correlated with $V_{\max}$ (Wullschleger 1993; Wohlfahrt et al. 1999; Medlyn et al. 1999), and its vertical profile has also

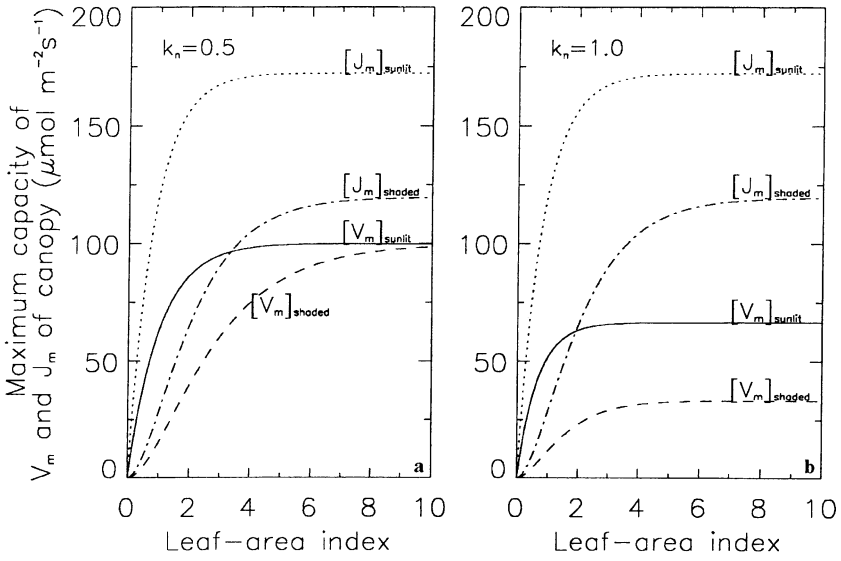

FIG. 3. Unstressed photosynthetic capacity, $[V_{max}]$ and $[J_{max}]$, as a function of leaf area index for sunlit/shaded fraction of canopy [Eqs. (38)–(41)] at the coefficient of nitrogen allocation: (a) $k_n = 0.5$, (b) $k_n = 1.0$.

been assumed to parallel to that of light (Wang and Polglase 1995; Wang and Leuning 1998). Based on these assumptions, the canopy values of $[V_{max}]$ and $[J_{max}]$ can be obtained by integrating from leaf to canopy, that is, Eqs. (37) and (38). Figure 3 shows the unstressed photosynthetic capacity of canopy, $[V_{max}]$ and $[J_{max}]$, over a range of leaf area index values. Here, $[V_{max}]$ and $[J_{max}]$ for sunlit leaves saturate at lower values of $L_{AI}(\sim 2)$ than that for shaded leaves ($L_{AI} \sim 5$). However, $[J_{max}]$ depends strongly on the assumed value of k_n. Both sunlit and shaded leaves have higher values of $[V_{max}]$ at the lower value of $k_n = 0.5$. Thus, with a more rapid decrease of leaf nitrogen concentration within the canopy, Rubisco activity is more likely to be limiting for the same top leaves.

For the assumed parameters, Fig. 4 shows that the shaded fraction of the canopy is always electron-transport-limited (i.e., $[w_e]_{j=2} < [w_c]_{j=2}$) and that the sunlit leaves are usually Rubisco-limited (i.e., $[w_c]_{j=1} < [w_e]_{j=1}$), except when the incident PAR is lower than 150 W m^{-2}.

Figure 5 shows the increase of assimilation in changing from very clear sky to totally diffuse radiation. The rate of assimilation saturates at lower values of PAR with a higher diffuse fraction. Hence, it has been suggested that diffuse radiation alone enhanced noontime photosynthesis of deciduous forests by 23% in 1992 and 8% in 1993 under cloudless conditions after the 1991 Mount Pinatubo eruption (Gu et al. 2003). Evidently, it is important to be able to distinguish between the direct and diffuse components. Although such data is usually not available in observations, it is readily generated by climate models.

3. Implementation with the common land model

The Common Land Model (CLM) has been developed for community use by a grass-roots collaboration of scientists who have an interest in making a general land model available for public use and further development (Dai et al. 2003). Its major model characteristics include: enough unevenly spaced layers to adequately represent soil temperature and soil moisture, and a multilayer parameterization of snow processes; an explicit treatment of the mass of liquid water and ice water and their phase change within the snow and soil system; a runoff parameterization following the Topography-based Runoff Prediction Model (TOPMODEL) concept; a canopy photosynthesis–conductance model that describes the simultaneous transfer of CO_2 and water vapor into and out of vegetation; a tiled treatment of subgrid fraction of energy and water balance. The CLM has been extensively evaluated in offline mode and by coupling runs with atmospheric models.

Its submodel of photosynthesis–stomatal conductance of CLM was directly adopted from the NCAR LSM (Bonan 1996), in which the $[A_n]$ and $[g_s]$ were calculated for the sunlit and shaded leaves using average absorbed PAR partitioned to sunlit and shaded leaves, but in which the calculation is applied a common energy budget equation and a common leaf temperature for sunlit and shaded leaves.

The original CLM code, has been modified to include a two-stream approximation scheme (Sellers 1985) (see appendix A) for a treatment of singularities. The subroutine for leaf temperature was rewritten for a nonlinear system of energy budget equations by the quasi-New-

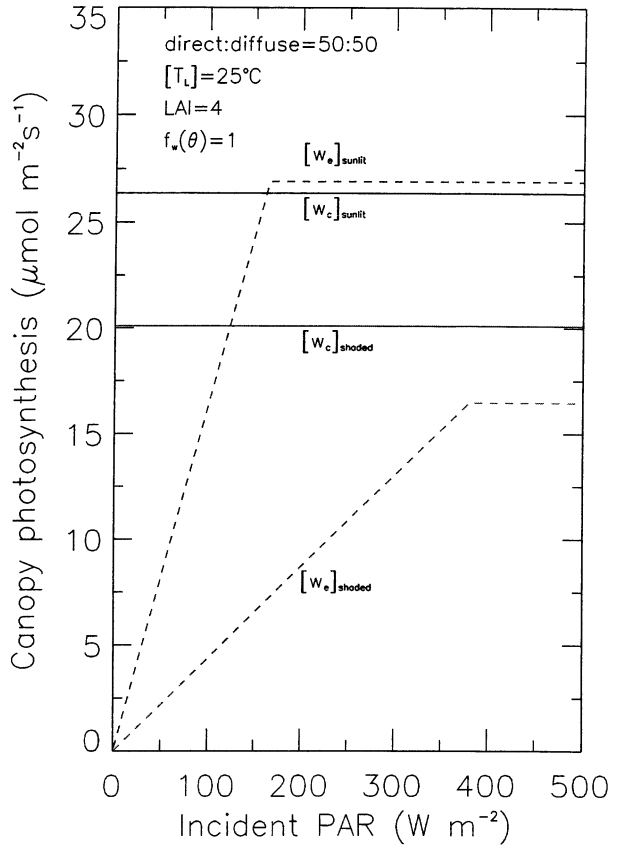

FIG. 4. Canopy rates of Rubisco-limited [w_c] and light-limited [w_e] as functions of incident PAR [Eqs. (22)–(23) with Eqs. (38)–(41)]. Values used in this calculation: 50% direct solar incident, 50% diffuse solar incident, $L_{AI} = 4$, leaf angle distribution is spherical, solar zenith angle is 0°, and soil water stress $f_w(\theta) = 1$, $[T_l]_{j=1} = [T_l]_{j=2} = 25$°C. Other parameters used are: $[c_i] = 24.5$ Pa, $c_m = 35$ Pa, $O_2 = 20\,900$ Pa, $\varepsilon = 0.08$, $k_n = 0.5$, $V_{cmax} = 100$ μmol m^{-2} s^{-1}.

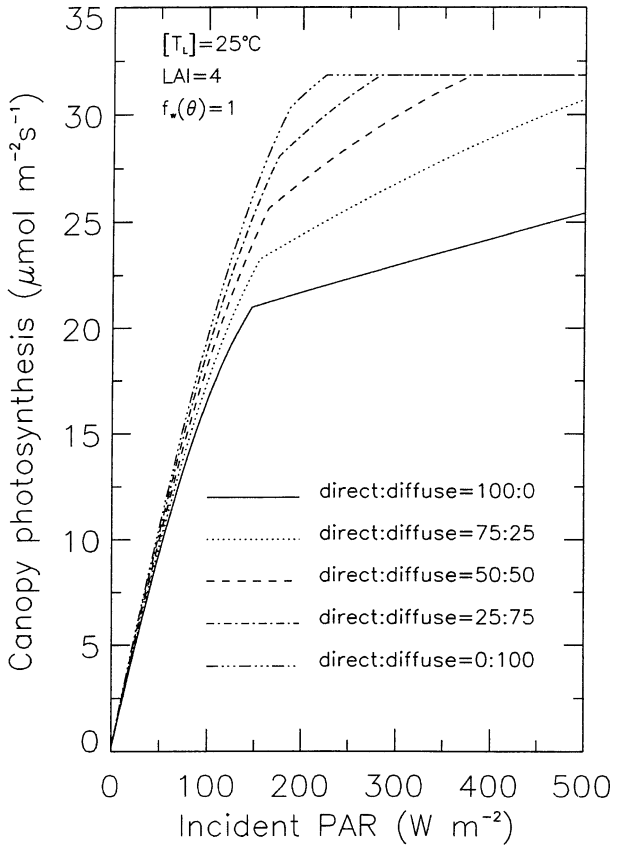

FIG. 5. Calculated effect of the fraction of direct/diffuse of incident PAR on canopy photosynthesis [A]. Values used in this calculation: $L_{AI} = 4$, leaf angle distribution is spherical, solar zenith angle is 0°, and soil water stress $f_w(\theta) = 1$, $[T_l]_{j=1} = [T_l]_{j=2} = 25$°C. Other parameters used are: $[c_i] = 24.5$ Pa, $c_m = 35$ Pa, $O_2 = 20\,900$ Pa, $\varepsilon = 0.08$, $k_n = 0.5$, $V_{cmax} = 100$ μmol m^{-2} s^{-1}.

ton–Raphson iteration method (see appendix C), the sequence of iteration calculations are listed as follows:

- aerodynamic resistance and bulk boundary layer resistance of leaves; heat conductance for air, leaf and ground;
- photosynthesis and stomatal conductance for sunlit fraction of canopy;
- photosynthesis and stomatal conductance for shaded fraction of canopy;
- leaf temperatures based on the energy balance equations;
- fluxes: CO_2, transpiration, evaporation, and sensible heat from leaves; and
- evaluation of stability-dependent variables using Monin–Obukhov length for next iteration.

The iteration stops at a convergence criterion of the energy budget residual and a small enough difference of leaf temperature between two iteration steps [Eqs. (C4) and (C5)].

4. Offline simulation with CLM

The runs were carried out for two forest sites using the observed meteorological forcing. For each case, the atmospheric forcing data for the first year are used for model spinup with soil water initialized at full saturation, both leaf and soil temperatures at the air temperature, and both snow depth and snow age at zero. The CLM were run with (i) two-big-leaf submodel (CLM 2L); (ii) one-big-leaf submodel (CLM 1L, appendix B); and (iii) NCAR LSM ($A_n - g_s$) scheme (i.e., CLM), respectively. The calculated CO_2 flux, sensible heat flux, latent heat flux, canopy photosynthesis rate, canopy stomatal conductance, and the leaf temperatures were compared with the observations.

a. Evergreen broadleaf forest (Reserva Jaru, Roddonia, Brazil)

The forcing data for the year 1992–93 were taken from the continued measurement by the automatic weather station at the top of the tower (52 m) at an undisturbed tropical rain forest at Reserva Jaru, Brazil (10.083°S,

TABLE 3. List of biome-dependent parameters used in the model for tropical evergreen broadleaf trees (TEBT) and northern old black spruce (NOBS). The V_{cmax} for TEBT is from Lloyd et al. (1995); V_{cmax} and ε for NOBS are from Dang et al. (1998) and Chen et al. (2000); other biochemical parameters are from Sellers et al. (1996b). Here, L_{AI} for TEBT is from Dai et al. (2003); for NOBS from Chen et al. (1997). The values bracketed are canopy averaged [V_{max}] used by CLM.

Parameters	TEBT	NOBS	Unit
V_{cmax}	68 (29.3*)	35** (15)	μmol m^{-2} s^{-1}
ε	0.08	0.021	mol mol^{-1}
m	9	9	—
b	0.01	0.01	mol m^{-2} s^{-1}
s_2	313	303	K
s_4	288	278	K
k_n	0.5	0.5	—
f_d	0.7	—	μmol m^{-2} s^{-1}

Leaf area index (L_{AI}, m^2 m^{-2})

	Jan	Feb	Mar	Apr	May	Jun	Jul	Aug	Sep	Oct	Nov	Dec
TEBT	4.48	4.09	3.74	3.68	3.68	3.68	3.68	3.68	3.68	3.85	4.36	4.60
NOBS	3.0	3.0	3.0	3.3	4.0	4.2	4.5	4.6	4.2	4.0	3.5	3.0

* The canopy averaged $\langle V_{max}\rangle$ derived from the $\langle V_{max}\rangle = V_{cmax}\{1 - \exp(-k_n\overline{L_t})\}/(k_n\overline{L_t})$, the annual averaged $\overline{L_t}$ was used (equal to 4.0).
** The V_{cmax} derived from $V_{cmax} = \langle V_{max}\rangle/(\{1 - \exp(-k_n\overline{L_t})\}/k_n\overline{L_t})$, the annual averaged $\overline{L_t}$ was used (equal to 3.7).

61.916°W). The measurements of the CO_2 flux, sensible and latent heat fluxes are for 8 days during the dry season (September 1992) and for 48 days during wet season (May–June 1993). An eddy covariance system mounted 15 m above the 30-m-tall forest was used to measure the fluxes over an area of about 1 km^2 (Grace et al. 1995). The same vegetation parameters are assumed for all three runs, the biome-dependent parameters are listed in Table 3. The soil respiration was taken as a constant 0.22 μmol m^{-2} s^{-1} in CLM 2L and CLM 1L runs.

Figures 6 and 7 show the averaged diurnal cycles of CO_2 flux, sensible and latent heat fluxes (above the canopy), CO_2 assimilation rate, canopy stomatal conductance and leaf temperatures over the dry season (8 days, September 1992) and the wet season (48 days, May–June 1993), respectively, by models and measurements. Positive value here for CO_2 flux indicates a net downward flux into the canopy. The observed CO_2 flux above the canopy shows net uptake during daylight and a nighttime efflux. A feature of two periods was the large spike of CO_2 leaving in the early morning. Photosynthesis was maximal in the first part of the morning, well before 1600 local time the canopy was typically in a state of carbon balance; during the night, respiration was 1–20 μmol m^{-2} s^{-1}. Except for the feature of CO_2 efflux in the early morning, CLM 1L and CLM 2L could reproduce most features in the measured fluxes. As expected, CLM 1L predicted higher values of CO_2 uptake, stomatal conductance, and hence related latent heat flux than did CLM 2L during the daytime. Bulk stomatal conductance predicted by CLM 1L and CLM 2L approach the peak value in the early morning, falling as the day progressed, which will match that obtained from measured evapotranspiration rates (Grace et al. 1996). Also as expected, CLM 2L predicted higher sunlit leaf temperature $[T_l]_{j=1}$ than the shaded $[T_l]_{j=2}$, the difference of the peak values are 3.4°C in the wet season and 4.3°C in the dry season. The leaf temperature by CLM 1L and by CLM are within the $[T_l]_{j=1}$ and $[T_l]_{j=2}$ and very close to $[T_l]_{j=2}$. Compared with CLM 1L and CLM 2L, the CLM shows performances that are very similar to that of CLM 1L.

All three runs failed to reproduce the observed spikes of CO_2 efflux above the canopy in the early morning, which were associated with the onset of turbulent conditions that followed calm nights. Typically, the natural ventilation of the canopy is poor at night, and respired CO_2 accumulates near the ground to over 500 ppmv (Grace et al. 1995). This disagreement might be from either. 1) inappropriate formulation of the plant or soil respiration; or 2) our neglect of storage or lateral transport of the CO_2 storage within the canopy or soil storage. The turbulence model used in the CLM and the overlying atmosphere should be as appropriate for other scalar transports as that of moisture.

There are not much differences in fluxes and temperatures between dry and wet season (Figs. 6 and 7) in both the observed and the simulated. There is good evidence to suggest that trees rely on deep roots in the dry seasons (Nepstad et al. 1994; Zeng et al. 1998; Dai et al. 2003).

Table 4 presented the comparison of mean values of fluxes and temperature over two full years by three runs. All numbers are as expected, that is, higher assimilation and latent heat flux, lower sensible heat flux and skin temperatures by CLM 1L compared to CLM.

b. Evergreen conifer forest (Thompson, Manitoba, Canada)

The site is near the northern edge of the boreal forest, in the zone of discontinuous permafrost (55.88°N, 98.48°W). The forcing data for 2-yr period of 18 January 1994–17 January 1996 were the average of two neighbor sites of the BOREAS Northern Study Area, which

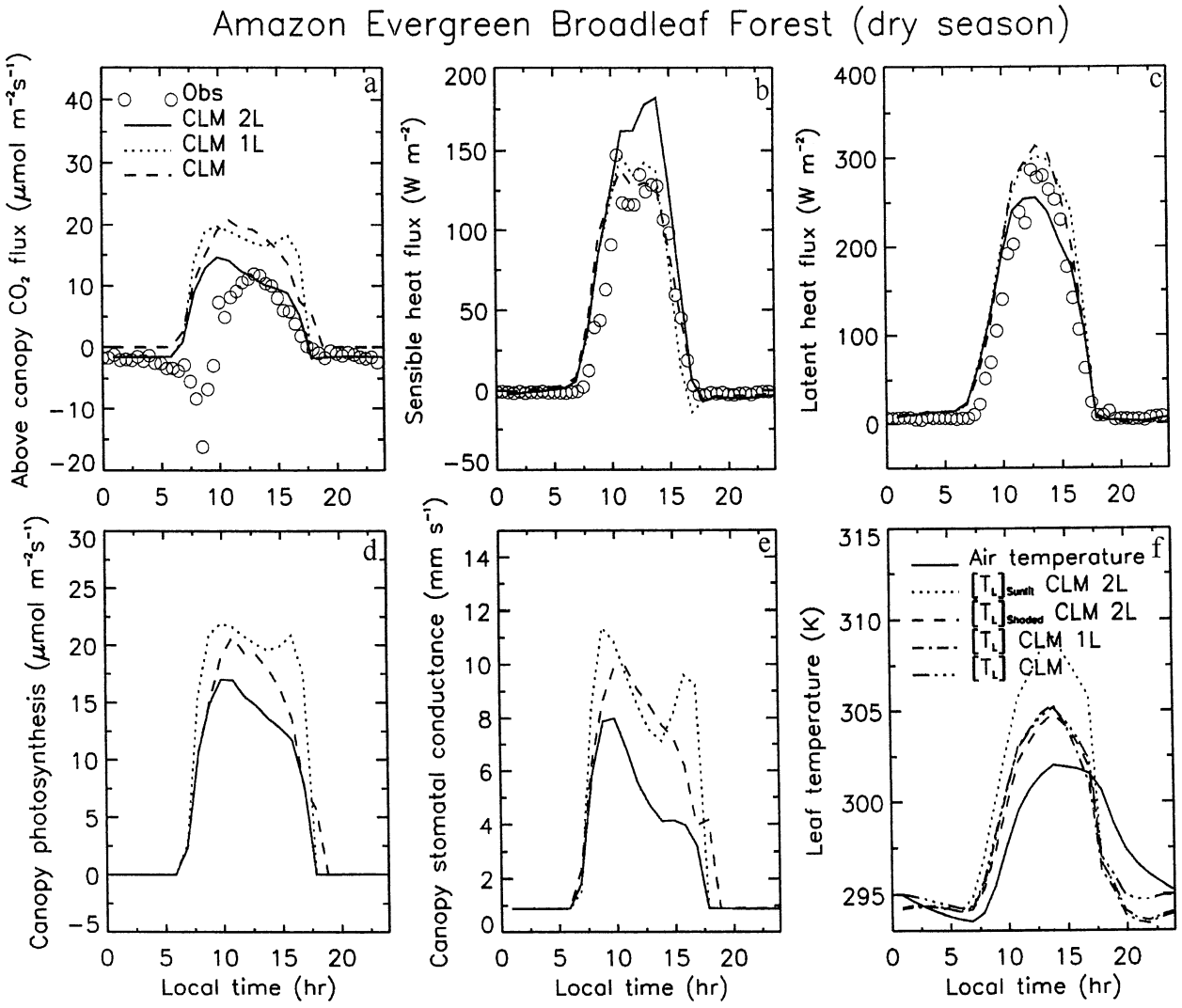

FIG. 6. Averaged diurnal variations of (a) net CO_2 flux, (b) sensible heat flux, (c) latent heat flux, (d) photosynthesis, (e) stomatal conductance, and (f) leaf temperatures over rainforest at Reserva Jaru in southwestern Amazonia during the dry season (7–14 Sep 1992) as observed and predicted by CLM with the two-big-leaf submodel (CLM 2L), CLM with the single-big-leaf submodel (CLM 1L), and CLM with LSM/NCAR scheme (CLM). Note that the CO_2 flux by CLM in (a) does not include the negative contribution from the respiration due to no calculation.

were quality checked by A. K. Betts. The eddy-correlation fluxes for CO_2 and H_2O were collected at a 30-m-tall tower that extends well above the canopy height of approximately 10-m-tall 120-year-old black spruce (Goulden et al. 1997). The same vegetation parameters are assumed for all three runs, the biome-dependent parameters for all three runs are listed in Table 3. The leaf and soil respirations in CLM 2L and CLM 1L runs are the fitted temperature-related equations from Lavigne et al. (1997): $R_d = 0.26 \exp\{0.07(T_L - 283.16)\}$, soil respiration: $R_{\text{soil}} = 0.6 \exp\{0.119(T_g - 273.16)\}$.

Figure 8 shows, as an example, the averaged diurnal cycles of CO_2 flux, sensible and latent heat fluxes (above the canopy), CO_2 assimilation rate, canopy stomatal conductance, and leaf temperatures over a period with the longest continuous recorded and high-quality observation (1 June–30 September 1994), by models and measurements. CLM 1L and CLM 2L provided a consistent performance as they did for the Amazon rainforest. CLM predicted lower assimilation rate and stomatal conductance, and hence, lower latent heat flux (Fig. 8 and Table 5), which are not consistent with that for the case of a tropical broadleaf forest. The underlying causes are unknown. But we quote the suspicion of Farquhar et al. (2001), ''there is a need to introduce penumbral effects, especially for coniferous species.''

5. Summary and discussion

Stomatal conductance exerts a major control on canopy transpiration. Its functioning is closely linked to the as-

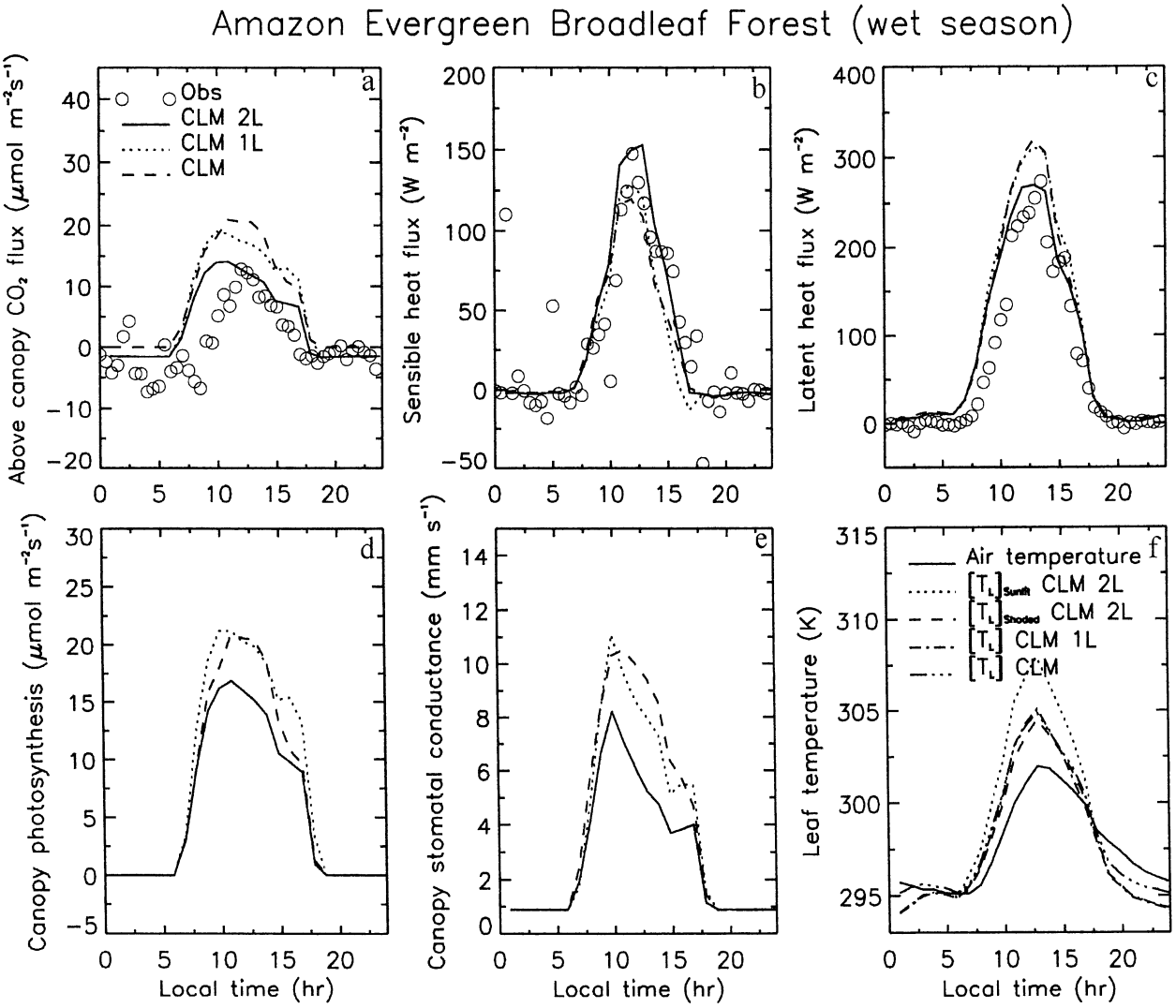

FIG. 7. Same as in Fig. 6, but for wet season (10 May–26 Jun 1993).

similation of carbon by leaves. Hence carbon assimilation models are used to parameterize stomatal conductance for climate models. The two-big-leaf model presented here improves previous such modeling by Collatz et al. (1991, 1992), Sellers et al. (1992, 1996a), Bonan (1996), de Pury and Farquhar (1997), Dickinson et al. (1998), and Dai et al. (2003) through the following:

1) separate treatments of sunlit and shaded leaves;
2) separate calculation of radiation absorption for sunlit and shaded leaves;
3) separate calculation of leaf temperatures, stomatal conductance, and fluxes (water, CO_2, and sensible heat) for sunlit and shaded fractions of canopy;
4) inclusion of exponential profiles for distribution of canopy photosynthetic capacity, and maximum potential electron transport rate;
5) use of soil water limitation for both maximum rates of RuBP carboxylation and electron transport;
6) separation of scaling up from leaf to canopy for sunlit and shaded fractions separately; the parameters of the canopy model have equivalent definitions and relationships between the leaf and canopy scales; and
7) coupled solution of the energy balance equations for sunlit and shaded leaf temperatures.

The functioning of these parameterizations has been tested in two 2-yr offline simulations with CLM. The simulations were reasonably successful in predicting the diurnal variation in leaf temperatures, canopy conductance, and fluxes (energy, CO_2, and water vapor). Consequences of altering the distribution of leaf nitrogen (Fig. 3), the density of incident of PAR (Fig. 4), and the fractions of diffuse and direct-beam radiation (Fig. 5) on canopy photosynthesis were also explored. This type of sensitivity analysis allows examination of the relative importance of various parameters of the model,

TABLE 4. Comparison of fluxes and temperatures simulated by CLM 2L, CLM 1L, and CLM. Mean values are 2-yr averages from 1 Jan 1992 to 31 Dec 1993 at Amazon rainforest site.

Variable	CLM 2L	CLM 1L	CLM	Unit
Sensible heat flux	46.4507	36.8699	35.9084	W m^{-2}
Latent heat flux	85.7762	98.0852	99.0203	W m^{-2}
Net radiation	132.249	134.931	134.893	W m^{-2}
Ground heat flux	−0.015 26	−0.016 52	−0.035 61	W m^{-2}
Assimilation rate	6.111 74	8.421 85	7.708 71	μmol m^{-2} s^{-1}
Respiration	2.183 00	2.053 12	0.0	μmol m^{-2} s^{-1}
Skin temperature	299.081	298.738	299.042	K
Leaf temperature	300.079*/298.688**	298.761	299.058	K

* Leaf temperature of sunlit fraction of canopy.
** Leaf temperature of shaded fraction of canopy.

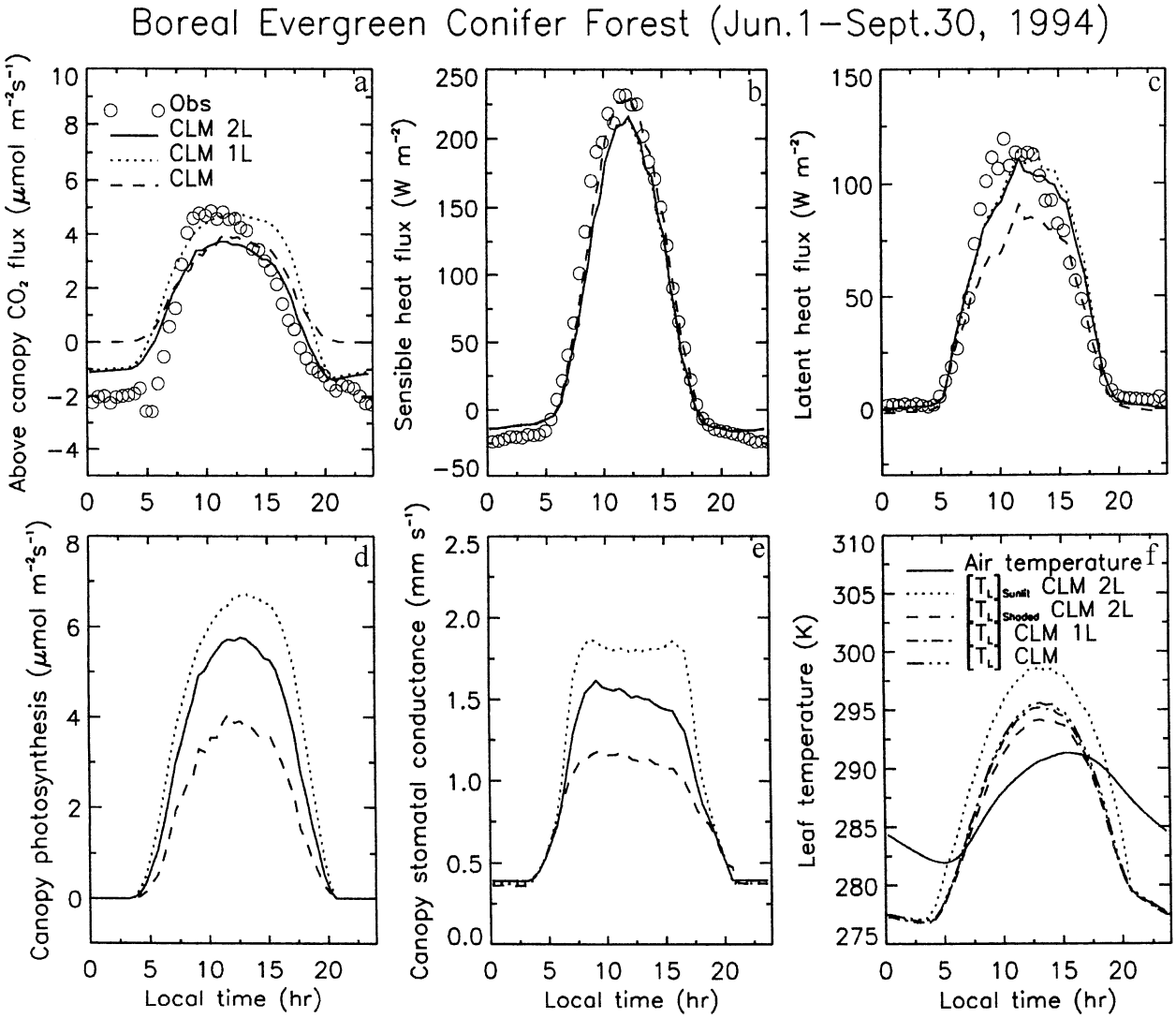

FIG. 8. Same as in Fig. 6 except over old black spruce at BOREAS/NOBS research site (1 Jun–30 Sep 1994). Also, the model averages are based on the time step values that are sampled only for the time step in which observation were taken.

TABLE 5. Comparison of fluxes and temperatures simulated by CLM 2L, CLM 1L, and CLM. Mean values are 2-yr averages from 18 Jan 1994 to 17 Jan 1996 at an old black spruce site of BOREAS/NOBS research.

Variable	CLM 2L	CLM 1L	CLM	Unit
Sensible heat flux	42.9223	43.1598	46.6155	W m^{-2}
Latent heat flux	22.0164	22.3806	18.3768	W m^{-2}
Net radiation	66.2251	66.8210	66.3250	W m^{-2}
Ground heat flux	1.297 13	1.296 97	1.333 34	W m^{-2}
Assimilation rate	0.954 117	1.128 56	0.786 453	μmol m^{-2} s^{-1}
Respiration	0.606 891	0.565 736	0.0	μmol m^{-2} s^{-1}
Skin temperature	269.466	269.346	269.455	K
Leaf temperature	271.201*/269.025**	269.335	269.436	K

* Leaf temperature of sunlit fraction of canopy.
** Leaf temperature of shaded fraction of canopy.

and hence, provides insight into the behavior of real plant canopies.

CLM 1L, which does not account for the difference in the radiation absorption and the difference of leaf temperature between sunlit leaves and shaded leaves, was found to give higher canopy fluxes (CO_2 and water vapor) than the CLM 2L. Vertical variation in leaf area index, fraction of diffuse beam radiation, and the leaf nitrogen content, preclude an accurate treatment of canopy photosynthesis with the one-leaf model (de Pury and Farquhar 1997). The two-big-leaf model presented here allows within-canopy profiles of the important leaf properties for carbon assimilation, and hence gives an accurate biochemically based model of photosynthesis.

CLM, which does not account for the difference of leaf temperature between sunlit leaves and shaded leaves, the varying of photosynthetic capacity with leaf area index L_{AI}, and the N distribution with canopy depth, was found to overestimate canopy fluxes (CO_2 and water vapor) for a tropical rainforest and underestimate them for the boreal conifer forest. CLM did use a fixed value of V_{max} at 25°C (i.e., include the nitrogen limitation in V_{max}, and does not allow the changes with L_{AI}), the V_{max} fitted at $L_{AI} = 4$ was 20% smaller than that at $L_{AI} = 2$ and even smaller at higher leaf area indices (at $k_n = 0.5$). For the plant with constant L_{AI} and uniform N distribution with canopy depth, the errors may be less important. However, it may be significant when L_{AI} is varying, such as in models that predict the response of vegetation to climate change.

Important aspects of canopy modeling not addressed here are: dependence of V_{max} on Rubisco, hence nitrogen cycling (Dickinson et al. 2002); plant and soil respiration; canopy turbulent transport of mass and energy.

Acknowledgments. This work has been supported by funding agencies including DOE to Georgia Institute of Technology, NASA through the IDS Program Grant (429-81-22; 428-81-22), and NSFC of China under Grant 40225013. We would like to acknowledge the assistance and helpful discussions from Alan Betts. We would also like to thank Niall Hanan and an anonymous reviewer for their thorough and constructive review. The ABRACOS data were collected under the ABRACOS project and made available by the Institute of Hydrology (United Kingdom) and the Instituto Nacional de Pesquisas Espaciais (Brazil); the BOREAS meteorological data were prepared by Alan Betts from the BOREAS CD-ROM, and the fluxes data were made available by the Steven C. Wofsy Group at Harvard University.

APPENDIX A

The Supplementaries to Two-Stream Approximation Radiative Transfer Model of Sellers (1985)

Radiative transfer within vegetation canopies is calculated from the two-stream approximation of Dickinson (1983) and Sellers (1985). The equations are as follows:

$$-\overline{\mu}\frac{dI^{\uparrow}}{dx} + \{1 - (1 - \beta)\omega\}I^{\uparrow} - \omega\beta I^{\downarrow} = \omega\overline{\mu}K\beta_0 \exp(-Kx) \quad \text{(A1)}$$

$$\overline{\mu}\frac{dI^{\downarrow}}{dx} + \{1 - (1 - \beta)\omega\}I^{\downarrow} - \omega\beta I^{\uparrow} = \omega\overline{\mu}K(1 - \beta_0) \exp(-Kx), \quad \text{(A2)}$$

where, $I^{\uparrow}$, $I^{\downarrow}$ are the upward and downward diffuse radiative fluxes, respectively, normalized by the incident flux; μ is the cosine of the zenith angle of incident beam; $G(\mu)$ is the projected area of phytoelements in direction μ; $\overline{\mu}$ is the average inverse diffuse optical depth per unit leaf area; K is the optical depth of the direct beam per unit leaf area, and $K = G(\mu)/\mu$; β, β_0 are the upscatter parameters for diffuse and direct beams; ω is the scattering coefficient of phytoelements;

The projected area in direction μ is given by

$$G(\mu) = \phi_1 + \phi_2\mu, \quad \text{(A3)}$$

where, $\phi_1 = 0.5 - 0.633\chi - 0.33\chi^2$, $\phi_2 = 0.877(1 - 2\phi_1)$, and χ is an empirical parameter related to the leaf angle distribution. The average inverse diffuse optical depth per unit leaf area is

$$\overline{\mu} = \int_0^1 \frac{\mu}{G(\mu)}\, d\mu = \frac{1}{\phi_2}\left\{1 - \frac{\phi_1}{\phi_2}\ln\left(\frac{\phi_1 + \phi_2}{\phi_1}\right)\right\}. \quad \text{(A4a)}$$

This integral is based on the assumptions: $\phi_1 \neq 0$ and $\phi_2 \neq 0$. Actually, ϕ_1 or ϕ_2 could be zero, the integral (A4a) does not work for these cases. We provide supplementary solutions as follows:

$$\overline{\mu} = 1/0.877, \quad \text{if } \phi_1 = 0 \quad \text{(A4b)}$$

$$\overline{\mu} = 1/(2\phi_1), \quad \text{if } \phi_2 = 0. \quad \text{(A4c)}$$

The analytic solutions of equations (A1) and (A2) provided by Sellers (1985) are strictly at $\sigma \neq 0$. We provide the solution for the singularity at $\sigma = 0$,

$$I^{\uparrow} = h_2' e^{-Kx} + h_3' e^{Kx} - \frac{h_1}{\overline{\mu}^2}\left(x + \frac{1}{2K}\right)e^{-Kx} \quad \text{(A5)}$$

$$I^{\downarrow} = h_5' e^{-Kx} + h_6' e^{Kx} + \frac{1}{c}\left\{-\frac{1}{2K}\frac{h_1}{\overline{\mu}^2}\left(p_3 x + p_4\frac{1}{2K}\right) - d\right\}e^{-Kx}. \quad \text{(A6)}$$

The coefficients are given by

$$b = \{1 - (1 - \beta)\omega\}$$

$$c = \omega\beta$$

$$d = \omega\overline{\mu}K\beta_0$$

$$f = \omega\overline{\mu}K(1 - \beta_0)$$

$$h = \frac{1}{\overline{\mu}}\sqrt{b^2 - c^2}$$

$$\sigma = \overline{\mu}^2K^2 - (b^2 - c^2)$$

$$h_1 = -dp_4 - cf$$

$$h_4 = -fp_3 - cd$$

$$p_1 = b + \overline{\mu}h$$

$$p_2 = b - \overline{\mu}h$$

$$p_3 = b + \overline{\mu}K$$

$$p_4 = b - \overline{\mu}K$$

$$S_1 = \exp(-hL_{\mathrm{AI}})$$

$$S_2 = \exp(-KL_{\mathrm{AI}})$$

$$m_1 = (1 - \alpha_{g,\mathrm{dif}}p_1/c)S_1$$

$$m_2 = (1 - \alpha_{g,\mathrm{dif}}p_2/c)/S_1$$

$$m_3 = \frac{h_1}{\overline{\mu}^2}\left(L_{\mathrm{AI}} + \frac{1}{2K}\right)S_2 + \alpha_{g,\mathrm{dif}}\frac{1}{c}\left\{-\frac{1}{2K}\frac{h_1}{\overline{\mu}^2}\left(p_3L_{\mathrm{AI}} + p_4\frac{1}{2K}\right) - d\right\}S_2 + \alpha_{g,\mathrm{dir}}S_2$$

$$n_3 = \frac{1}{4K^2}\frac{h_1}{\overline{\mu}^2}p_4 + d$$

$$h_2' = (m_3p_2 - m_2n_3)/(m_1p_2 - m_2p_1)$$

$$h_3' = (m_3p_1 - m_1n_3)/(m_2p_1 - m_1p_2)$$

$$h_5' = h_2'p_1/c$$

$$h_6' = h_3'p_2/c.$$

APPENDIX B

One-Big-Leaf Model

The leaf temperatures are determined by the canopy energy budget equations:

$$C_c\frac{\partial[T_l]}{\partial t} = 0 = [I_s] + [I_{\mathrm{ir}}] - [H_c] - L[E_c]. \quad \text{(B1)}$$

Here, [ ] denotes the integration canopy, that is, $\int_0^{L_{\mathrm{AI}}}[\ ]\,dx$, the sensible heat flux H_c and LE_c latent heat flux from foliages to canopy air are given, respectively,

$$[H_c] = \rho c_p L_{\mathrm{AI}}\frac{[T_l] - T_{\mathrm{af}}}{r_b} \quad \text{(B2)}$$

$$L[E_c] = L\left\{\rho(1 - f_{\mathrm{wet}})\delta_1 L_{\mathrm{AI}}\frac{1}{r_b + r_s} + \rho f_{\mathrm{wet}}(L_{\mathrm{AI}} + S_{\mathrm{AI}})\frac{1}{r_b}\right\} \times \{q_{\mathrm{sat}}([T_l]) - q_{\mathrm{af}}\}. \quad \text{(B3)}$$

Here, r_s is the averaged leaf stomatal resistance for sunlit and shaded. The radiation absorbed by leaves of the canopy are given by,

$$[I_s] = \int_0^{L_{\mathrm{AI}}}\{I_{\mathrm{lb}} + (I_{\mathrm{lbs}} + I_{\mathrm{ld}})\}\,dx \quad \text{(B4)}$$

$$[I_{\mathrm{ir}}] = \delta_t(I_{\mathrm{at}} - 2\sigma[T_l]^4 + \sigma T_g^4). \quad \text{(B5)}$$

The CO_2 flux budget within canopy can be described by the CO_2 concentration conservation equation:

$$C_{\mathrm{CO_2}}\frac{\partial c_a}{\partial t} = 0 = -F_c - [A_n] + R_p + R_{\mathrm{soil}}. \quad \text{(B6)}$$

The scheme of $[A_n - g_s]$ is similar to the two-big-leaf submodel, but the integrations of Eqs. (19)–(27) over canopy are for single big-leaf. The canopy values of $V_{\max}$ and $J_{\max}$ are given by

$$[V_{\max}] = \int_0^{L_{\mathrm{AI}}} V_{\max}(x)\,dx = V_{c\max}(1 - e^{-k_nL_{\mathrm{AI}}})\frac{1}{k_n} \quad \text{(B7)}$$

$$[J_{\max}] = \int_0^{L_{\mathrm{AI}}} J_{\max}(x)\,dx = J_{c\max}(1 - e^{-k_{d,1}^*L_{\mathrm{AI}}})\frac{1}{k_{d,1}^*}. \quad \text{(B8)}$$

APPENDIX C

Numerical Scheme for Leaf Temperatures

The equations of leaf temperatures [Eq. (5)] can be written as a two-dimensional vector-valued function whose components are the individual equations to be satisfied simultaneously, that is,

$$F_1([T_l]_{j=1}, [T_l]_{j=2}) = 0$$
$$F_2([T_l]_{j=1}, [T_l]_{j=2}) = 0. \quad \text{(C1)}$$

The numerical solutions are given by quasi-Newton–Raphson method as follows:

$$[\delta T_l]_{j=1} = -\frac{F_1^n \partial F_2/\partial [T_l]_{j=2} - F_2^n \partial F_1/\partial [T_l]_{j=2}}{\partial F_1/\partial [T_l]_{j=1}(\partial F_2/\partial [T_l]_{j=2}) - (\partial F_1/\partial [T_l]_{j=2})\partial F_2/\partial [T_l]_{j=1}}$$
$$[\delta T_l]_{j=2} = -\frac{F_1^n \partial F_2/\partial [T_l]_{j=1} - F_2^n \partial F_1/\partial [T_l]_{j=1}}{\partial F_1/\partial [T_l]_{j=2}(\partial F_2/\partial [T_l]_{j=1}) - (\partial F_1/\partial [T_l]_{j=1})\partial F_2/\partial [T_l]_{j=2}}, \quad \text{(C2)}$$

where the superscript n denotes the number of the iteration step, δ, here, is the difference in iteration step $n + 1$ and n. The convergent criterions for iteration are

$$\|F\| = \sqrt{F_1^2 + F_2^2} < 0.1, \quad \text{and} \quad \text{(C3)}$$
$$\|X\| = \sqrt{[\delta T_l]_{j=1}^2 + [\delta T_l]_{j=2}^2} < 0.01. \quad \text{(C4)}$$

APPENDIX D

List of Symbols Used in Paper

A	Leaf assimilation rates (mol m^{-2} s^{-1})
A_n	Net leaf assimilation (mol m^{-2} s^{-1})
b	Minimum stomatal conductance (mol m^{-2} s^{-1})
c_a, c_s, c_i	Partial pressure of CO_2 in canopy air, at the leaf surface and interior leaf, respectively (pa)
c_m	Partial pressure of CO_2 in atmosphere reference height (pa)
c_p	Specific heat of air (J kg^{-1} K^{-1})
E_a	Flux of water from canopy air
e_a, e_s, e_i	Partial pressure of H_2O in canopy air space, at the leaf surface and inside the leaf, respectively (pa)
E_c	Water vapor flux (including transpiration and interception loss) from leaves to canopy air (kg m^{-2} s^{-1})
E_g	Water vapor flux from the ground
E_{tr}	Transpiration (kg m^{-2} s^{-1})
f_d	Leaf respiration factor
F_c	CO_2 flux from canopy to atmosphere
f_{root}	Root fraction within soil layer
F_{Sha}	Fraction of shaded leaves of the canopy
f_{sha}	Fraction of shaded leaves at canopy depth
F_{Sun}	Fraction of sunlit leaves of the canopy
f_{sun}	Fraction of sunlit leaves at canopy depth x
$f_T(T_l)$	Temperature dependence of V_m or J_{max}
$f_w(\theta)$	Soil moisture dependence of V_m or J_{max}
f_{wet}	Fraction of wetted leaves of the canopy
g_a	Aerodynamic conductance of water vapor between reference height and canopy air space
g_b	Canopy stomatal conductance
g_s	Bulk canopy boundary layer conductance
g_l	Leaf boundary conductance (mol m^{-2} s^{-1})
g_s	Leaf stomatal conductance (mol m^{-2} s^{-1})
$G(\mu)$	Projected area of phytoelements in direction of the sun
H_a	Sensible heat flux from canopy to atmosphere (W m^{-2})
H_c	Sensible heat flux from foliages to canopy air (W m^{-2})
H_g	Sensible heat flux from the ground (W m^{-2})
h_s	Relative humidity at leaf surface
I_{b0}	Incident direct beam (W m^{-2})
I_{d0}	Incident diffuse beam (W m^{-2})
$I_{dif}^{\downarrow}$	Downward diffuse fluxes of diffuse incident solar multiscattered by leaves and ground, normalized by the incident diffuse solar flux
$I_{dif}^{\uparrow}$	Upward diffuse fluxes of diffuse incident solar multiscattered by leaves and ground, normalized by the incident diffuse solar flux
$I_{dir}^{\downarrow}$	Downward diffuse fluxes of the direct incident solar scattered by leaves and ground normalized by the incident direct solar flux
$I_{dir}^{\uparrow}$	Upward diffuse fluxes of the direct incident solar scattered by leaves and ground, normalized by the incident direct solar flux
I_{ir}	Net absorbed thermal radiation for sunlit leaves (W m^{-2})
I_{lb}	Absorbed direct incident beam—without scattering (W m^{-2})
I_{lbs}	Absorbed diffusion radiation scattered by leaves for direct incident beam (W m^{-2})
I_{ld}	Absorbed diffuse incident beam (W m^{-2})
I_s	Net solar radiation absorbed by sunlit/shaded fraction of canopy (W m^{-2})
J_m	Potential electron transport (mol m^{-2} s^{-1})

J	Electron transport rate (mol m^{-2} s^{-1})
$J_{c\max}$	Leaves at the top of the canopy at 25°C (mol m^{-2} s^{-1})
$J_{\max}$	Maximum (light-saturated) electron transport rate (mol m^{-2} s^{-1})
k_b	Direct-beam solar extinction coefficient of canopy
K_c	Rubisco Michaels–Menten constant for CO_2 (pa)
$k^*_{d,1}$	Extinction coefficients for diffuse PAR
k_n	Coefficient of leaf nitrogen allocation within canopy
K_o	Rubisco inhibition constant for oxygen (pa)
L_a	Incident thermal infrared radiation (mol m^{-2} s^{-1})
L_{AI}	Leaf area index (m^2 m^{-2})
L_{sha}	Leaf area index of shaded fraction of canopy (m^2 m^{-2})
L_{Sun}	Leaf area index of sunlit fraction of canopy (m^2 m^{-2})
m	Stomatal slope factor
N	Leaf nitrogen
N_0	Nominal leaf nitrogen content at the top of the canopy
N_{I}	Leaf nitrogen concentration
N_b	A residual leaf nitrogen content (a threshold value of leaf nitrogen content below which there is no photosynthesis) when $V_{\max} = 0$
O_2	Partial pressure of O_2 in leaf interior (pa)
p	Atmospheric pressure at surface (pa)
Q_{10}	Q_{10} temperature coefficient
q_{af}	Specific humidity of canopy space air (kg kg^{-1})
$q_{\mathrm{sat}}(T_l)$	Saturated specific humidity (kg kg^{-1}) at temperature T_l
R	Universal gas constant, 8.314 J mol^{-1} K^{-1}
r_b	Leaf boundary layer resistance (s m^{-1})
R_d	Dark respiration rate (mol m^{-2} s^{-1})
R_p	Nonleaf plant respiration (mol m^{-2} s^{-1})
r_s	Leaf stomatal resistance (s m^{-1})
R_{soil}	CO_2 flux from soil surface to canopy air
S	Rubisco specificity for CO_2 relative to oxygen (pa)
s_1	Slope of high temperature inhibition function (K^{-1})
s_2	One-half point of high temperature inhibition function (K)
s_3	Slope of low temperature inhibition function (K^{-1})
s_4	One-half point of low temperature inhibition function (K)
s_5	Slope of high temperature inhibition function (leaf respiration) (K^{-1})
s_6	One-half point of high temperature inhibition function (leaf respiration) (K)
S_{AI}	Dead leaf or stem area index
T_{af}	Temperature of canopy space air (K)
T_g	Ground temperature (K)
T_l	Leaf temperatures
$V_{c\max}$	Maximum rubisco capacity at top canopy at 25°C per leaf area (mol m^{-2} s^{-1})
V_m	Maximum catalytic capacity of Rubisco at saturating levels of Ribulose bisphosphate (RuBP) and intercellular partial pressure of CO_2, (mol m^{-2} s^{-1})
$V_{\max}$	Maximum rate of carboxylation
w_c	Rubisco (leaf enzyme) limited rate of assimilation (mol m^{-2} s^{-1})
w_e	Light-limited rate of assimilation (mol m^{-2} s^{-1})
w_s	Carbon compound export limitation (C_3 plants), or PEP-carboxylase (C_4) limitation on photosynthesis (mol m^{-2} s^{-1})
μ	Cosine of solar zenith angle
ρ	Density of air (kg m^{-3})
θ	Solar zenith angle, soil volumetric content
σ	Stefan–Boltzmann constant (W m^{-2} K^{-4})
χ	Empirical parameter related to the leaf angle distribution
ε	Intrinsic quantum yield epsilon (mol mol^{-1})
Γ^*	CO_2 compensation point (pa)
δ_1, δ_2	Step functions for sunlit and shaded leaves
δ_t	Fraction of longwave absorbed by canopy
ψ_{fc}	Soil matrix potential at filled capacity (mm)
$\psi_{\max}$	Soil matrix potential before leaf desiccation (mm)
χ_n	Ratio of Rubisco capacity to leaf nitrogen

REFERENCES

Ball, J. T., 1988: An analysis of stomatal conductance. Ph.D. thesis, Stanford University, 89 pp.

Boardman, N. K., 1977: Comparative photosynthesis of sun and shaded plants. *Ann. Rev. Plant Physiol.,* **28,** 355–377.

Bonan, G. B., 1996: A land surface model (LSM version 1.0) for ecological, hydrological, and atmospheric studies: Technical description and user's guide. NCAR Tech. Note NCAR/TN-417+STR, 150 pp.

Chen, J. M., P. M. Rich, S. T. Gower, J. M. Norman, and S. Plummer, 1997: Leaf area index of boreal forests: Theory, techniques, and measurements. *J. Geophys. Res.,* **102D,** 29 429–29 443.

Chen, W., J. Chen, J. Liu, and J. Cihlar, 2000: Approaches for reducing uncertainties in regional forest carbon balance. *Global Biogeochem. Cycles,* **14,** 827–838.

Collatz, G. J., J. T. Ball, C. Grivet, and J. A. Berry, 1991: Physiological and environmental regulation of stomatal conductance, photosynthesis, and transpiration: A model that includes a laminar boundary layer. *Agric. For. Meteor.,* **54,** 107–136.

——, M. Ribas-Carbo, and J. A. Berry, 1992: Coupled photosynthesis–stomatal conductance model for leaves of C4 plants. *Aust. J. Plant Physiol.,* **19,** 519–538.

Dai, Y., and Coauthors, 2003: The Common Land Model (CLM). *Bull. Amer. Meteor. Soc.,* **84,** 1013–1023.

Dang, Q.-L., H. A. Margolis, and G. J. Collatz, 1998: Parameterization and testing of a coupled photosynthesis–stomatal conductance model for boreal trees. *Tree Physiol.,* **18,** 141–153.

de Pury, D. G. G., and G. D. Farquhar, 1997: Simple scaling of photosynthesis from leaves to canopy without the errors of big-leaf models. *Plant Cell Environ.,* **20,** 537–557.

Dickinson, R. E., 1983: Land surface processes and climate-surface

albedos and energy balance. *Advances in Geophysics,* Vol. 25, Academic Press, 305–353.
——, A. Henderson-Sellers, P. J. Kennedy, and M. F. Wilson, 1993: Biosphere–atmosphere transfer scheme (BATS) version 1e as coupled for Community Climate Model. NCAR Tech. Note NCAR/TN-378+STR, 72 pp.
——, M. Shaikh, R. Bryant, and L. Graumlich, 1998: Interactive canopies for a climate model. *J. Climate,* **11,** 2823–2836.
——, and Coauthors, 2002: Nitrogen controls on climate model evapotranspiration. *J. Climate,* **15,** 278–295.
Farquhar, G. D., and S. C. Wong, 1984: An empirical model of stomatal conductance. *Aust. J. Plant Physiol.,* **11,** 191–210.
——, S. von Caemmerer, and J. A. Berry, 1980: A biochemical model of photosynthetic CO_2 assimilation in leaves of C3 plants. *Planta,* **147,** 78–90.
——, S. von Caemmerer, and J. A. Berry, 2001: Models of photosynthesis. *Plant Physiol.,* **125,** 42–45.
Field, C. B., 1983: Allocating leaf nitrogen for the maximization of carbon gain: Leaf age as a control on the allocation program. *Oecologia,* **56,** 341–347.
Goudriaan, J., and H. H. van Laar, 1994: *Modeling Potential Crop Growth Processes.* Kluwer Academic Publishers, 238 pp.
Goulden, M. L., B. C. Daube, S.-M. Fan, and D. J. Sutton, 1997: Physiological responses of a black spruce forest to weather. *J. Geophys. Res.,* **102** (D24), 29 987–28 997.
Grace, J., and Coauthors, 1995: Carbon dioxide uptake by an undisturbed tropical rain forest in South-West Amazonia, 1992–1993. *Science,* **270,** 778–780.
——, J. Lloyd, J. Mclntyre, A. C. Miranda, P. Meir, and H. S. Miranda, 1996: Carbon dioxide flux over Amazon rain forest in Rondonia. *Amazon Deforestation and Climate,* J. H. C. Gash et al., Eds., John Wiley, 307–318.
Gu, L., D. D. Baldocchi, S. C. Wofsy, J. W. Munger, J. J. Michalsky, S. P. Urbanski, and T. A. Boden, 2003: Response of a deciduous forest to the Mount Pinatubo eruption: Enhanced photosynthesis. *Science,* **299,** 2035–2038.
Harley, P. C., R. B. Thomas, J. F. Reynolds, and B. R. Strain, 1992: Modelling photosynthesis of cotton grown in elevated CO_2. *Plant Cell Environ.,* **15,** 271–282.
Hirose, T., and M. J. A. Werger, 1987: Maximising daily canopy photosynthesis with respect to the leaf nitrogen allocation pattern in the canopy. *Oecologia,* **72,** 520–526.
Kucharik, C. J., J. M. Norman, and S. T. Gower, 1998: Measurements of leaf orientation, light distribution and sunlit leaf area in a boreal aspen forest. *Agric. For. Meteor.,* **91,** 127–148.
Lavigne, M. B., and Coauthors, 1997: Comparing nocturnal eddy covariance measurements to estimates of ecosystem respiration made by scaling chamber measurements at six coniferous boreal sites. *J. Geophys. Res.,* **102** (D24), 28 977–28 985.
Leuning, R., R. N. Cromer, and S. Rance, 1991: Spatial distribution of foliar nitrogen and phosphorus in crowns of *Eucalyptus grandis. Oecologia,* **88,** 504–510.
——, F. M. Kelliher, D. G. G. Pury, and E.-D. Schulze, 1995: Leaf nitrogen, photosynthesis, conductance and transpiration: Scaling from leaves to canopies. *Plant Cell Environ.,* **18,** 1183–1200.
Lloyd, J., and Coauthors, 1995: A simple calibrated model of Amazon rainforest productivity based on leaf biochemical properties. *Plant Cell Environ.,* **18,** 1129–1145.
McNaughton, K. G., 1994: Effective stomatal and boundary resistances of heterogeneous surfaces. *Plant Cell Environ.,* **17,** 1061–1068.
Medlyn, B. E., and Coauthors, 1999: Effect of elevated [CO_2] on photosynthesis in European forest species: A meta-analysis of model parameters. *Plant Cell Environ.,* **22,** 1475–1495.
Nepstad, D. C., and Coauthors, 1994: The role of deep roots in the hydrological and carbon cycles of Amazonian forests and pastures. *Nature,* **372,** 666–669.
Norman, J. M., 1979: Modeling the complete crop canopy. *Modification of the Aerial Environment of Crops,* B. J. Barfield and J. Gerber, Eds., American Society of Agricultural Engineers, 249–277.
Raupach, M. R., 1995: Vegetation–atmopshere interaction and surface conductance at leaf, canopy and regional scales. *Agric. For. Meteor.,* **73,** 151–180.
Sellers, P. J., 1985: Canopy reflectance, photosynthesis and transpiration. *Int. J. Remote Sens.,* **6,** 1335–1372.
——, J. A. Berry, G. J. Collatz, C. B. Field, and F. G. Hall, 1992: Canopy reflectance, photosynthesis, and transpiration. III. A reanalysis using improved leaf models and a new canopy integration scheme. *Remote Sens. Environ.,* **42,** 187–216.
——, and Coauthors, 1996a: A revised land surface parameterization (SiB2) for atmospheric GCMs. Part I: Model formulation. *J. Climate,* **9,** 676–705.
——, S. O. Los, C. J. Tucker, C. O. Justice, D. A. Dazlich, G. J. Collatz, and D. A. Randall, 1996b: A revised land surface parameterization (SiB2) for Atmospheric GCMs. Part II: The generation of global fields of terrestrial biophysical parameters from satellite data. *J. Climate,* **9,** 706–737.
Sinclair, T. R., C. E. Murphy, and K. R. Knoerr, 1976: Development and evaluation of simplified models for simulating canopy photosynthesis and transpiration. *J. Appl. Ecol.,* **13,** 813–829.
Smith, E., 1937: The influence of light and carbon dioxide on photosynthesis. *J. Gen. Physiol.,* **20,** 807–830.
Spitters, C. J. T., H. A. J. M. Toussaint, and J. Goudriann, 1986: Separating the diffuse and direct component of global radiation and its implications for modeling canopy photosynthesis. Part I. Components of incoming radiation. *Agric. For. Meteor.,* **38,** 225–230.
Tezara, W., V. J. Mitchell, S. D. Driscoll, and D. W. Lawlor, 1999: Water stress inhibits plant photosynthesis by decreasing coupling factor and ATP. *Nature,* **401,** 914–917.
Wang, Y.-P., 2000: A refinement to the two-leaf model for calculating canopy photosynthesis. *Agric. For. Meteor.,* **101,** 143–150.
——, 2003: A comparison of three different canopy radiation models commonly used in plant modelling. *Funct. Plant Biol.,* **30,** 143–152.
——, and P. J. Jarvis, 1990: Description and validation of an array model—MAESTRO. *Agric. For. Meteor.,* **51,** 257–280.
——, and ——, 1993: Influence of shoot structure on photosynthesis of Sitka spruce (*Picea sichensis*). *Funct. Ecol.,* **7,** 433–451.
——, and P. J. Polglase, 1995: Carbon balance in the tundra, boreal forest and humid tropical forest during climate change: Scaling up from leaf physiology and soil carbon dynamics. *Plant Cell Environ.,* **18,** 1226–1244.
——, and R. Leuning, 1998: A two-leaf model for canopy conductance, photosynthesis and portioning of available energy I: Model description and comparison with a multi-layered model. *Agric. For. Meteor.,* **91,** 89–111.
——, ——, H. A. Cleugh, and P. A. Coppin, 2001: Parameter estimation in surface exchange models using non-linear inversion: How many parameters can we estimate and which measurements are most useful? *Global Change Biol.,* **7,** 495–510.
Wohlfahrt, G., M. Bahn, E. Haubner, I. Horak, W. Michaeler, K. Rottmar, U. Tappeiner, and A. Cemusca, 1999: Inter-specific variation of the biochemical limitation to photosynthesis and related leaf traits of 30 species from mountain grassland ecosystems under different land use. *Plant Cell Environ.,* **22,** 1281–1296.
Woods, D. B., and N. C. Turner, 1971: Stomatal response to changing light by four tree species of varying shaded tolerance. *New Phytol.,* **70,** 77.
Wullschleger, S. D., 1993: Biochemical limitations to carbon assimilation in C_3 plants—A retrospective analysis of A/ci cuves for 109 species. *J. Exp. Botany,* **44,** 907–920.
Zeng, X., Y. Dai, R. E. Dickinson, and M. Shaikh, 1998: The role of root distributions for land climate simulation. *Geophys. Res. Lett.,* **25,** 4533–4536.